



Leptin acts in the carotid bodies to increase minute ventilation during wakefulness and sleep and augment the hypoxic ventilatory response

Candela Caballero-Eraso^{1,2}, Mi-Kyung Shin¹, Huy Pho¹, Lenise J Kim^{1,3}, Luis E. Pichard¹, Zhi-Juan Wu¹ , Chenjuan Gu¹, Slava Berger¹, Luu Pham¹, Ho-Yee (Bonnie) Yeung⁴, Machiko Shirahata^{4,*}, Alan R. Schwartz¹, Wan-Yee (Winnie) Tang⁴, James S. K. Sham¹ and Vsevolod Y. Polotsky¹ 

¹Division of Pulmonary and Critical Care Medicine, Department of Medicine, Johns Hopkins University School of Medicine, Baltimore, MD, USA

²Unidad Médico-Quirúrgica de Enfermedades Respiratorias, Instituto de Biomedicina de Sevilla (IBiS), Centro de Investigación Biomédica en Red de Enfermedades Respiratorias (CIBERES), Hospital Universitario Virgen del Rocío/Universidad de Sevilla, Sevilla, Spain

³Departamento de Psicobiología, Universidade Federal de São Paulo, São Paulo, Brazil

⁴Department of Environmental Health and Engineering, Johns Hopkins Bloomberg School of Public Health, Baltimore, MD, USA

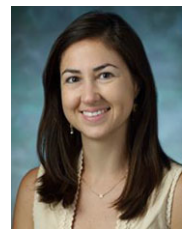
Edited by: Harold Schultz & Benedito Machado

Key points

- Leptin is a potent respiratory stimulant.
- A long functional isoform of leptin receptor, *LepR^b*, was detected in the carotid body (CB), a key peripheral hypoxia sensor. However, the effect of leptin on minute ventilation (V_E) and the hypoxic ventilatory response (HVR) has not been sufficiently studied.
- We report that *LepR^b* is present in approximately 74% of the CB glomus cells.
- Leptin increased carotid sinus nerve activity at baseline and in response to hypoxia *in vivo*.
- Subcutaneous infusion of leptin increased V_E and HVR in C57BL/6J mice and this effect was abolished by CB denervation.
- Expression of *LepR^b* in the carotid bodies of *LepR^b* deficient obese *db/db* mice increased V_E during wakefulness and sleep and augmented the HVR.
- We conclude that leptin acts on *LepR^b* in the CBs to stimulate breathing and HVR, which may protect against sleep disordered breathing in obesity.

Abstract Leptin is a potent respiratory stimulant. The carotid bodies (CB) express the long functional isoform of leptin receptor, *LepR^b*, but the role of leptin in CB has not been fully elucidated. The objectives of the current study were (1) to examine the effect of subcutaneous leptin infusion on minute ventilation (V_E) and the hypoxic ventilatory response to 10% O₂ (HVR) in C57BL/6J mice before and after CB denervation; (2) to express *LepR^b* in CB of *LepR^b*-deficient obese *db/db* mice and examine its effects on breathing during sleep and wakefulness and on HVR. We found that leptin enhanced carotid sinus nerve activity at baseline and in response to 10% O₂

Candela Caballero Erasó's research focuses on understanding the role of the carotid body in the setting of intermittent hypoxia/sleep apnoea with special interest in its regulatory mechanisms modifying specific cardiovascular or respiratory responses. Candela received her degree in Medicine from the Faculty of Medicine, University of Extremadura, in 2007 and her MD, PhD in 2015 from the University of Seville. Since 2013 she has combined her clinical activity as a specialist in respiratory medicine at the University Hospital Virgen del Rocío with her biomedical research at the Institute of Biomedicine of Seville and the Johns Hopkins University in Baltimore, USA.



*Deceased

in vivo. In C57BL/6J mice, leptin increased V_E from 1.1 to 1.5 mL/min/g during normoxia ($P < 0.01$) and from 3.6 to 4.7 mL/min/g during hypoxia ($P < 0.001$), augmenting HVR from 0.23 to 0.31 mL/min/g/ ΔF_{IO_2} ($P < 0.001$). The effects of leptin on V_E and HVR were abolished by CB denervation. In *db/db* mice, *LepR^b* expression in CB increased V_E from 1.1 to 1.3 mL/min/g during normoxia ($P < 0.05$) and from 2.8 to 3.2 mL/min/g during hypoxia ($P < 0.02$), increasing HVR. Compared to control *db/db* mice, *LepR^b* transfected mice showed significantly higher V_E throughout non-rapid eye movement (20.1 vs. -27.7 mL/min respectively, $P < 0.05$) and rapid eye movement sleep (16.5 vs 23.4 mL/min, $P < 0.05$). We conclude that leptin acts in CB to augment V_E and HVR, which may protect against sleep disordered breathing in obesity.

(Resubmitted 27 July 2018; accepted after revision 3 October 2018; first published online 4 October 2018)

Corresponding author V. Y. Polotsky, MD, PhD: Professor of Medicine, Division of Pulmonary and Critical Care Medicine, Department of Medicine, The Johns Hopkins University School of Medicine, 5501 Hopkins Bayview Circle, Johns Hopkins Asthma and Allergy Center, Rm 4B65, Baltimore, MD 21224, USA. Email: vpolots1@jhmi.edu

Introduction

The body has several compensatory mechanisms in response to hypoxia. One of these is the ability to increase ventilation, which is called the hypoxic ventilatory response (HVR) (Teppema & Dahan, 2010). The HVR is a complex phenomenon. Peripheral sensing of hypoxia occurs predominantly in the carotid bodies (CB), which are located in the carotid artery bifurcation with the aortic bodies playing a secondary role. The CB glomus (type I) cells sense hypoxia and transmit chemosensory input via the carotid sinus nerve (CSN), a branch of the glossopharyngeal nerve, to the nucleus of the solitary tract (NTS) and to the brainstem respiratory network (Gonzalez-Martin *et al.* 2011; Silva & Schreihofner, 2011; Prabhakar *et al.* 2012; Nurse & Piskuric, 2013; Prabhakar, 2013). The HVR is time dependent and the isocapnic HVR can be divided in two phases, a first phase (0–5 min) of hyperventilation followed by a second phase of a slow decline (5–20 min). The first phase is predominantly peripheral governed by the CB activity and the initial 1–2 min is exclusively peripheral, whereas both peripheral and central chemoreception contribute to the second phase (Powell *et al.* 1998; Duffin, 2007; Teppema & Dahan, 2010).

Abnormal HVR plays an important role in the pathogenesis of sleep disordered breathing (SDB), which is one of the most common complications of obesity. Obstructive sleep apnoea, i.e. recurrent closure of the upper airway during sleep, is observed in >50% of obese individuals (Tufik *et al.* 2010; Peppard *et al.* 2013), and is associated with an abnormally augmented HVR (Younes *et al.* 2007; Pialoux *et al.* 2009; Trombetta *et al.* 2013; Younes, 2014; Mateika, 2015). Obesity may also lead to alveolar hypoventilation during sleep due to respiratory depression, which can be present independent of obstructive sleep apnoea (Mokhlesi, 2010). Obesity hypoventilation is characterized by suppressed HVR (Zwillich *et al.* 1975). The mechanisms by which obesity affects the HVR are not fully understood.

Recent reports suggest that the CB express receptors for leptin. Leptin is an adipocyte-produced hormone, levels of which increase exponentially with increased obesity (Maffei *et al.* 1995; Considine *et al.* 1996). *LepR^b*, the longest isoform of leptin receptor (*LepR*) primarily responsible for leptin signalling (Chen *et al.* 1996), is abundantly expressed in the CB (Porzionato *et al.* 2011; Messenger & Ciriello, 2013; Messenger *et al.* 2013; Ciriello & Caverson, 2014). Leptin acts in medullary centres to regulate responses to hypercapnia (O'Donnell *et al.* 1999; Inyushkina *et al.* 2010; Bassi *et al.* 2012, 2014; Yao *et al.* 2016). Leptin deficiency causes central alveolar hypoventilation and obstructive sleep apnoea in rodents (O'Donnell *et al.* 1999; Polotsky *et al.* 2001, 2012; Pho *et al.* 2016; Yao *et al.* 2016) and may predispose obese humans to sleep apnoea (Shapiro *et al.* 2014). Leptin increases minute ventilation (V_E) in rats and mice during normoxia (O'Donnell *et al.* 1999; Yao *et al.* 2016; Ribeiro *et al.* 2018) and during hypoxic exposure (Ribeiro *et al.* 2018; Yuan *et al.* 2018) and augments CSN activity in response to anoxia *ex vivo* (Shirahata *et al.* 2015; Ribeiro *et al.* 2018). In awake lean Zucker rats, leptin did not change baseline V_E , but increased HVR and the effect of leptin on HVR was abolished by CB denervation (Yuan *et al.* 2018). However, many aspects of leptin's action remain unknown. It is unclear if leptin acts in the CB to augment baseline V_E or only the HVR and whether leptin regulates CSN activity *in vivo* during exposure to physiologically relevant levels of hypoxia. The role of leptin's action in the CB in the pathogenesis of obesity-induced SDB is unknown.

We hypothesized that leptin acts in the CB to increase the HVR and minute ventilation during sleep and wakefulness. We elucidated the effects of leptin in the CB by several complementary approaches. First, we examined the effects of intravenous leptin on CSN activity during 100% hyperoxia, when CB are inactivated, and in response to 10% O_2 hypoxia *in vivo* in C57BL/6J mice. Second, we performed continuous infusion of leptin in lean C57BL/6J

mice, raising its levels to the values observed in obese mice and measured minute ventilation and the HVR in unanaesthetized unrestrained animals before and after CNS dissection (CSND). Third, we expressed *LepR^b* in the CB of *LepR^b*-deficient obese *db/db* mice and evaluated minute ventilation and HVR during wakefulness and breathing during sleep.

Methods

Ethical approval

All animal surgical procedures were done using aseptic techniques under 1–2% isoflurane anaesthesia. After survival surgeries, mice were housed in a recovery chamber, and their behaviour was monitored. Buprenorphine 0.05–0.1 mg/kg (SQ) was administered as required based on signs of distress or pain (e.g. audible noises, no movement, eating or drinking behaviours). Upon completion of the experimental protocols or in case of ill appearance and/or persistent distress mice were killed under isoflurane anaesthesia by an overdose of pentobarbital (60 mg i.p.). The study was approved by the Johns Hopkins University Animal Use and Care Committee (Protocols MO15M257 and MO16M161) and complied with the American Physiological Society Guidelines for Animal Studies.

Animals and overall design

In total, 42 adult male C57BL/6J mice (Stock #000664), 30 adult male *db/db* mice on the C57BL/6J background (Stock #000697) 8–10 weeks of age, from the Jackson Laboratory (Bar Harbor, MA, USA), and five male *LepR^b-EGFP* mice were used in our experiments. *LepR^b-EGFP* mice were generated by breeding *LepR^b-Cre* [B6.129(Cg)-Lep^{rtm2}(cre)Rck/J, Stock #008320] and enhanced green fluorescent protein (EGFP) reporter mice [B6;129-Gt(ROSA)26Sortm2Sho/J, Stock #004077] from the Jackson Laboratory. All mice had free access to food and water and were housed under standard laboratory conditions at 22°C with the 12:12-h light–dark cycle (0900–2100 h lights on/2100–0900 h lights off). C57BL/6J mice were used for the HVR measurements ($n = 17$), for arterial blood gas (ABG) measurements ($n = 7$) and for CSN activity measurements ($n = 18$, including ten mice treated with leptin and eight mice treated with vehicle, i.e. saline). For the HVR experiments, mice were acclimatized for 4–7 days to the plethysmography chamber. A subcutaneous osmotic pump (DURECT, Cupertino, CA, USA) filled with saline was implanted and after 2 days of recovery, the HVR was measured (see the HVR protocol below). Subsequently, a subcutaneous osmotic pump for leptin infusion (120 μ g/day for 2 days) was implanted and 48 h later the HVR was measured. After this,

CSND ($n = 12$) or CSND sham surgery ($n = 5$) was performed and, after 5–7 days of recovery, the HVR was determined following the same protocol (Fig. 1A). Weight, temperature and food intake were measured during leptin and saline infusions and blood samples were taken by retro-orbital puncture under 1–2% isoflurane anaesthesia to measure leptin levels in plasma. *LepR^b* receptor deficient *db/db* mice were used for the HVR experiment before and after virus infection ($n = 15$), for sleep studies ($n = 10$) and for staining and CB morphometry ($n = 5$). For the HVR, mice were acclimatized for 3–5 days to the plethysmography chamber, and baseline measurements were then taken. Subsequently, the CB area was infected with *Ad-LacZ* ($n = 6$) or *Ad-LepR^b* ($n = 9$) adenoviral vectors (see protocol below) and the HVR measurements were repeated over 15 days and blood samples were taken to measure plasma leptin levels. Sleep studies were performed 15 days after *Ad-LacZ* ($n = 5$) and after *Ad-LepR^b* infections ($n = 5$).

Carotid sinus nerve dissection protocol

CSND was performed as previously described by our group (Shin *et al.* 2014) with modifications. Briefly, the surgery was performed under 1–2% isoflurane anaesthesia and body temperature was maintained at 37°C. The CSNs were bilaterally dissected and painted with a solution of 2% phenol diluted in ethanol at the points of branching from the glossopharyngeal nerve to the cranial pole of the CB. To prevent discomfort, buprenorphine at 0.05 mg/kg/day s.c. was administered. Mice recovered for at least 5–7 days. Sham surgery was performed in a similar manner except that the CSNs were not severed.

Ad-LacZ and *Ad-LepR* infection of the CB area in *db/db* mice

For the leptin receptor long *LepR^b* isoform expression in the CB, *db/db* mice were anaesthetized with 2% isoflurane, and the carotid artery bifurcation areas were carefully exposed bilaterally. The adenovirus harbouring the *LepR^b* gene (*Ad-LepR^b*) or control virus *Ad-LacZ*, provided by Dr Christopher Rhodes (University of Chicago) were suspended in Matrigel matrix (BD Biosciences, Bedford, MA, USA) at 1:5 and 5 μ L of the viral suspension was applied to the CB area bilaterally at a final concentration of 0.86×10^{12} plaque-forming units (pfu)/mL. Following this procedure, skin was re-apposed and the incision was carefully closed. The HVR measurements were performed 15 days later, allowing for recovery and adenovirus expression in the CB area. In addition, five *db/db* mice were transfected with *Ad-LepR^b-GFP* (Vector Biolabs, Malvern, PA., USA; $2\text{--}5 \times 10^{10}$ pfu/mL) for morphometry.

Arterial blood gases experiment

An arterial catheter was implanted in the left femoral artery under 1–2% isoflurane anaesthesia. The femoral artery was carefully exposed via a 0.5 cm incision and an arterial catheter was inserted 5–8 mm deep into the femoral artery, glued in place and routed under the skin. The skin was sutured with 6.0 silicon-coated silk sutures. The catheter was attached to a single-channel fluid swivel (model 375/25, Instech Laboratories, Plymouth Meeting,

PA, USA) and perfused slowly by an infusion pump (0.5 mL/day) with a sterile saline solution containing heparin (1000 U heparin/L saline). Mice were allowed to recover for a minimum of 48 h prior to blood gas testing, which was performed in awake anaesthetized unrestrained mice removing 150 μ L of arterial blood, which was processed in a blood analyser (Radiometer ABL 800 Flex, Diamond Diagnostics, Holliston, MA, USA). The alveolar–arterial gradient for partial pressure of O₂ ($P_{A}O_2 - P_{a}O_2$) was calculated at room air conditions

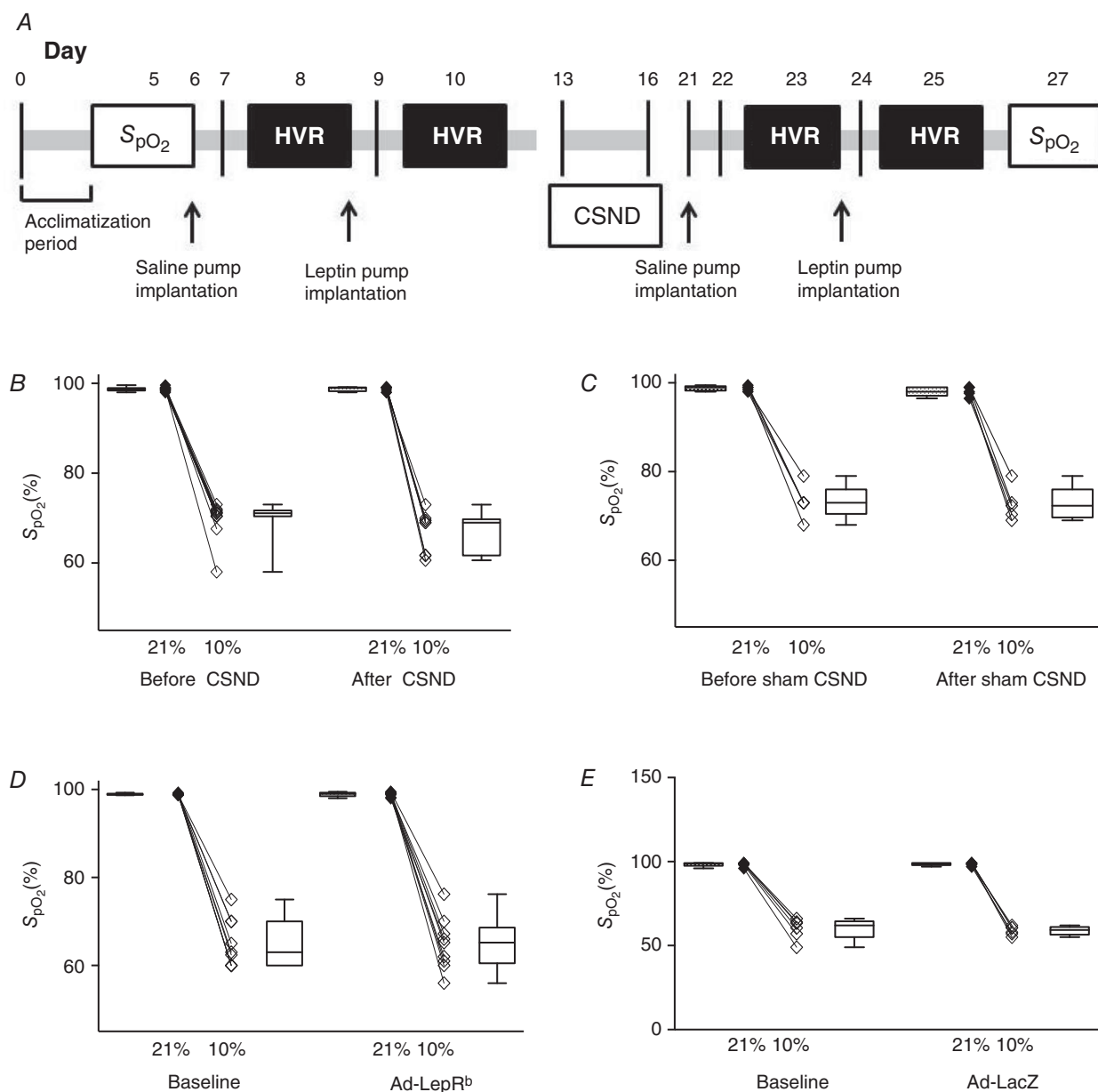


Figure 1. The effect of leptin on the hypoxic ventilatory response in C57BL/6J mice

A, experimental design of the hypoxic ventilatory response (HVR) experiment in C57BL/6J mice before and after subcutaneous leptin infusion via an osmotic pump (120 μ g/day) before and after carotid sinus nerve denervation (CSND); **B** and **C**, oxyhaemoglobin saturation (S_{pO_2}) in C57BL/6J mice exposed to normoxia and hypoxia before and after CSND ($n = 9$, **B**) or sham surgery ($n = 5$, **C**); **D** and **E**, S_{pO_2} in *db/db* mice exposed to normoxia and hypoxia at baseline and after carotid body area infection with *Ad-LacZ* ($n = 6$, **D**) or *Ad-LepR^b* ($n = 9$, **E**).

before and after CSND ($n = 7$) assuming that $P_{A}O_2 = F_{IO_2} (P_{atm} - P_{H_2O}) - P_{aCO_2}/0.8$.

Body temperature measurements

Body temperature was measured at 10.00 h after overnight acclimation to thermoneutral conditions by a rectal probe in awake C57BL/6J mice at baseline and during saline and leptin infusions and in *db/db* mice before and 15 days after *Ad-LepR^b* or *Ad-LacZ* control CB infection. Body temperature measurements were repeated before and after the HVR measurements and sleep studies.

Pulse oximetry

Oxyhaemoglobin saturation (S_{pO_2}) was measured by pulse oximetry in 10% and 20.9% O_2 by applying a Mouse CollarClip (Starr Life Sciences, Oakmont, PA, USA).

Minute ventilation and the hypoxic ventilatory response

HVR measurements were performed at thermoneutral conditions (30°C) in a neonatal incubator (Draeger 8000 IC), which has been adapted for respiratory and metabolic measurements in our laboratory (Jun *et al.* 2013). Mice were acclimatized overnight prior to the measurements. Tidal volume (V_T), respiratory rate and minute ventilation (V_E) were measured in C57BL/6J mice before and after CSND during saline and leptin infusions, and in *db/db* mice before and after virus infection as previously described (Polotsky *et al.* 2001, 2004) with modifications according to Hernandez *et al.* (2012). The methodology of our ventilatory measurements has been previously described in detail (Hernandez *et al.* 2012). Briefly, the animals were placed in a whole body barometric plethysmography (WBP) chamber (Buxco, Wilmington, NC, USA) with internal diameter of 80 mm, height of 50.5 mm and volume approximately of 0.4 L. The chamber consisted of a sealed animal chamber, a reference chamber and a platform inside the chamber to support the mouse (Pho *et al.* 2016). The chamber was equipped with two high-resistance ports on the upper surface and one large side port and three small side ports at the base. The inflow and outflow high-resistance ports were connected to positive and negative pressure sources to generate a steady bias flow through the mouse chamber preventing CO_2 accumulation. The bias flow inlet and outlet ports were adjusted to maintain chamber at atmospheric pressure and to keep the time constant of the chamber much longer than the inspiratory time of the animal, thereby preventing pressure leakage during respiration (Hernandez *et al.* 2012). This approach, based on previous work (Pappenheimer, 1977; Jacky, 1978), allowed us to use the chamber as if it was completely sealed. The Drorbaugh and Fenn equation was used to

calculate WBP tidal volume signal from the WBP chamber pressure signal (Drorbaugh & Fenn, 1955). Application of this formula required measurement of the following variables during each WBP recording session: mouse rectal temperature, chamber temperature, room temperature and relative humidity, and chamber gas constant, which was calculated by utilizing a known-volume injection and the resultant WBP pressure deflection. Calibration injections of fixed 1 mL volume of room air were made with the animal inside the constant-volume chamber. All signals were digitized at 1000 Hz (sampling frequency per channel) and recorded in LabChart 7 Pro (version 7.2). WBP pressure was recorded with a differential pressure transducer (no. 3613, Emka Technologies, Falls Church, VA, USA). A first-order derivative (dV/dt) was applied to the WBP tidal volume signal to yield a WBP tidal airflow signal (Hernandez *et al.* 2012). All respiratory measurements in our systems were previously validated against gold standard pneumotachographic measures of tracheal pressure in anaesthetized mice (Hernandez *et al.* 2012).

During both normoxia (20.9% O_2) and hypoxia (10% $O_2 + 3\% CO_2$), air flow was constant and was regulated by the mass flow controller. Once the chamber was at constant volume, V_T (tidal volume) and respiratory rate (RR) were derived from changes in pressure (Statham Gould PM15E differential pressure transducer, Hato Ray, Puerto Rico). Minute ventilation (\dot{V}_E) was reported as ($V_T \times RR$)/body weight and was measured during quiet wakefulness at baseline, 20.99% O_2 for 25 min three times at least 30 min apart, and in response to 10% $O_2 + 3\% CO_2$ for 5 min three times at least 30 min apart. To eliminate inhibitory effects of hypocapnia on the HVR, we used a 10% O_2 and 3% CO_2 mixture for our measurements. During normoxia F_{IO_2} was 20.9% and CO_2 was 0.4%. After switching to hypoxia, F_{IO_2} decreased to 10% and CO_2 increased to 3% within a 30 s interval.

In C57BL/6J mice, the HVR was measured before and after CSND or sham surgery and in *db/db* mice, it was measured before and after *Ad-LacZ* or *Ad-LepR^b* infection. Relationships between F_{IO_2} and S_{pO_2} in C57BL/6J mice before and after CSND or sham surgery are presented in Fig. 1B and C, and the same relationships in *db/db* mice before and after *Ad-LacZ* or *Ad-LepR^b* infection are presented in Fig. 1D and E. In C57BL/6J mice, the bulk of the osmotic pump prevented accurate S_{pO_2} measurements during leptin or saline infusion. Therefore, the HVR was calculated as the ratio of [V_E (10% O_2) - V_E (20.9% O_2)] to the change in F_{IO_2} ($\Delta F_{IO_2} = 10.9\%$ between normoxia and hypoxia) and reported as $\Delta V_E/\Delta F_{IO_2}$. In *db/db* mice, the HVR was reported both as $\Delta V_E/\Delta F_{IO_2}$ and as a ratio of [V_E (10% O_2) - V_E (20.9% O_2)] the change in oxyhaemoglobin saturation (S_{pO_2} (20.9% O_2) - S_{pO_2} (10% O_2)] and reported as $\Delta V_E/\Delta S_{pO_2}$. Given that the peripheral chemoreflex is more brisk and predominates during the

Table 1. Arterial blood gas values in awake unrestrained C57BL/6J mice exposed to 21% O₂ and 10% O₂ + 3% CO₂ before and after carotid sinus nerve dissection

	Intact carotid bodies		Carotid sinus nerve dissection	
	21% O ₂	10% O ₂ + 3% CO ₂	21% O ₂	10% O ₂ + 3% CO ₂
pH	7.4 ± 0.01	7.4 ± 0.01	7.4 ± 0.02	7.4 ± 0.001
P _{O₂} (mmHg)	96.0 ± 4.6	52.3 ± 2.9	106.5 ± 7.7	53.0 ± 10.4
P _{CO₂} (mmHg)	28.1 ± 1.5	29.7 ± 1.5	31.3 ± 0.9	29.07 ± 0.7

Results are presented as mean ± SEM.

first 2 min of hypoxic exposure (Powell *et al.* 1998; Teppema & Dahan, 2010; Duffin, 2007), we reported values during the first 2 min of hypoxic exposure. We also performed ABG measurements at normoxic conditions and during the first 2 min of hypoxic exposure to ensure isocapnoea during hypoxic exposure. In mice with intact and denervated CB, ABG showed similar levels of partial pressure of CO₂ (P_{aCO₂}) at normoxic and hypoxic conditions (Table 1).

Sleep studies

EEG and EMG electrodes were implanted with an EEG/EMG Headmount (Pinnacle Technology, Lawrence, KS, USA) as previously described (Pho *et al.* 2016). Mice were allowed to recover for 3–4 days prior to polysomnography in a designated room where sleep recordings were later performed. This climate control sound-proof room had a constant temperature of 27–28°C and the 12:12 h light-dark cycle (lights on 09.00–21.00 h/lights off 21.00–09.00 h). Animals were placed in a modified whole body plethysmography open-system chamber designed to record tidal airflow, respiratory effort and sleep-wake state continuously (Hernandez *et al.* 2012) as described above. During full polysomnographic recording sessions, the chamber was humidified to 90% relative humidity. Mice were habituated to the WBP chamber from 10.00 to 16.00 h 1 day before the recording session and 45 min to acclimatize to the chamber before recordings were initiated on the day of recording. Sleep recordings were performed for 6 h during the light phase (10.00 to 16.00 h). Tidal volume and respiratory movements were measured as described above, and EEG/EMG signals were recorded as previously described (Pho *et al.* 2016; Fleury Curado *et al.* 2018).

Sleep-wake state was scored visually in 5-s epochs from 10.00 to 16.00 h. Standard criteria were employed to score sleep-wake state based on EEG and EMG frequency content and amplitude, as previously described (Pho *et al.* 2016). Studies were scored by two independent scorers (CCE and HP), who were blinded to study conditions. Wakefulness was characterized by low-amplitude, high-frequency (~10 to 20 Hz) EEG waves and high levels of EMG activity compared with

the sleep states. Non-rapid eye movement (NREM) sleep was characterized by high-amplitude, low-frequency (~2–5 Hz) EEG waves with EMG activity considerably less than during wakefulness. Rapid eye movement (REM) sleep was characterized by low-amplitude, mixed-frequency (~5–10 Hz) EEG waves with EMG amplitude either below or equal to that during NREM sleep.

Ventilation was assessed by V_E and its components, tidal volume and respiratory rate, during non-flow-limited and flow-limited breathing. Obstruction was characterized by the development of inspiratory flow limitation as previously described (Pho *et al.* 2016). Briefly, the severity of airflow obstruction was defined by maximal inspiratory flow at the onset of flow limitation (V_Imax), measured at the point of peak inspiratory airflow. Breaths were considered to be flow limited if (1) breaths had an early peak of inspiratory flow followed by a plateau or a decrease in flow, (2) a mid-inspiratory plateau occupied ≥20% of inspiratory time between early and late inspiratory peaks in flow, or (3) when the late inspiratory airflow peak exceeded the early peak (Pho *et al.* 2016). Mean S_{pO₂} characterized the severity of gas exchange abnormalities across sleep/wake states. Because sleep stage can markedly affect SDB severity, we stratified analyses by NREM vs. REM sleep. The oxygen desaturation index (ODI) was defined as ≥ 4% oxyhaemoglobin desaturation from the baseline (ODI) for at least two breaths. We also measured the frequency of sighs defined as breaths with amplitude exceeding two tidal volumes as an indicator of respiratory control stability during sleep (Yamauchi *et al.* 2008).

Measurements of CSN activity in ventilated mice

Mice were anaesthetized with urethane 1.25 g kg⁻¹ (i.p.) and ventilated via a tracheal tube by a modified volume-controlled Harvard animal ventilator (Model 687, Harvard Apparatus, Holliston, MA, USA) under hyperoxia (100% O₂) as previously described (Tankersley *et al.* 1994; Pichard *et al.* 2015). The right common carotid artery was cannulated for monitoring blood pressure and the right jugular vein was cannulated for leptin infusion. Subsequently, for neuromuscular blockade mice were given pancuronium bromide (0.03–0.04 mg kg⁻¹, i.p.). The neck

was dissected to expose the left carotid bifurcation and the glossopharyngeal nerve. CSN was identified and the central end was sectioned. The area including the CB and CSN was filled with Krebs solution. The sectioned end was then placed into a glass suction pipette containing a silver–silver chloride electrode and Krebs solution. Additionally, a silver–silver chloride electrode was placed in the surrounding solution to serve as the ground electrode. The signal was amplified (AC-Preamplifier P15, Grass Instruments Co., West Warwick, RI, USA) and collected using digital recording software (AcqKnowledge, BioPac Systems, Inc., Goleta, CA, USA) together with airway pressure and arterial pressure. Baroreceptors were mechanically denervated in a manner similar to those previously described (Shirahata & Fitzgerald, 1991; Van Vliet *et al.* 1999). Successful removal of baroreceptors was confirmed when increased blood pressure did not accompany an increase in CSN activity. Functional viability of the CB and CSN was assessed prior to the experiment and at the end by a brief exposure to 100% inspired N₂, which leads to a vigorous increase in nerve activity. Following confirmation of a viable preparation, mice were left undisturbed for 5 min under hyperoxic conditions (100% O₂). Following this 5-min baseline, two hypoxic challenges (10% O₂) of 90 s were performed with a 5-min inter-challenge period for recovery under hyperoxic conditions. Following the second hypoxic challenge and 5-min recovery period, intravenous leptin (3 µg in 300 µL of saline over 45–60 s) was given and allowed to stabilize under hyperoxic conditions for 10 min. Following this stabilization period the above-mentioned protocol was repeated to test hypoxic responses under leptin. Control experiments were conducted in a similar fashion expect that the same volume of saline was infused over the same time instead of leptin. For the analysis, each continuous 120-s challenge (15-s baseline, 90-s challenge and 15-s post-challenge recovery period) was filtered using both low-pass and high-pass window-based filters of 1000 and 250 Hz, respectively. Filters were selected based on data presented by Pichard, *et al.* (2015), which demonstrated that this approach would adequately capture the activity of the *in vivo* murine CSN activity in response to 10% hypoxia. Subsequently, nerve activity in each continuous challenge was broken down into adjacent 5-s segments. Signal in each segment was then detrended, rectified and finally integrated. The maximum of the integrated signal represents the total neural activity for each 5-s segment. For each hypoxic period, the sum of all 5-s segments was taken as total neural output for the hypoxic challenge.

Plasma leptin levels

Plasma leptin levels in C57BL/6J and *db/db* mice were measured by Mouse Leptin ELISA kits (catalogue number EZML_82K) from Millipore (Billerica, MA, USA).

Immunohistochemistry in tissue sections

Mice were anaesthetized with 1–2% isoflurane and perfused transcardially using 500 mL ice-cold phosphate buffered saline (PBS; 0.01 M, pH 7.4) followed by 4% paraformaldehyde (PF) in 0.1 M PBS. The carotid artery bifurcations with the CB were removed bilaterally, kept for 2 h in PF 4%, washed in PBS 0.1 M, cryoprotected in PBS with 30% sucrose and embedded in Tissue-Tek O.C.T. compound, and frozen on dry ice. Coronal cryosections of 10 µm were obtained on Superfrost plus slides (Thermo Scientific, Waltham, MA, USA) using a cryostat (HM 560, Thermo Scientific) and tissue was stored at –20°C. For staining, cryosections were brought to room temperature for 10 min and then rehydrated with PBS. Antigen retrieval was subsequently performed using sodium citrate buffer (10 mM sodium citrate, 0.05% Tween 20, pH 6.0) at 95°C for 20 min followed by three washes for 10 min with PBS with 0.3% Triton X-100. The sections were blocked at room temperature with 10% normal goat serum, 1% bovine serum albumin, 20 µL Triton X-100 and 10 µL Tween 20 for 1 h followed by incubation with primary antibodies diluted in blocking solution overnight at 4°C. On the following day, sections were washed with PBS with 0.1% Triton X-100 and incubated with the secondary antibodies for 1 h at room temperature and washed with PBS. Then, slides were coverslipped with mounting medium for fluorescence with DAPI (4,6-diamidino-2-phenylindole; Vectashield, Vector Labs, Burlingame, CA, USA).

LepR^b protein expression in the CB of *LepR^b-EGFP* mice was detected based on the presence of a reporter, EGFP (Scott *et al.* 2009). LepR^b protein expression in *LepR^b-deficient db/db* mice after infection with *Ad-LepR^b* was also detected based on the presence of the reporter. We used tyrosine hydroxylase (TH) as a type I cell marker and glial fibrillary acidic protein (GFAP) as a type II cell marker (Lopez-Barneo *et al.* 2009) For the anti-TH staining in *LepR^b-EGFP* and in *db/db* transfected mice we used a chicken anti-TH primary antibody (Abcam 1:500, catalogue number ab76442; Cambridge, MA, USA) and goat anti-Chicken IgY secondary antibody, Alexa Fluor 568 (1:500, catalogue number A-11041). For GFAP we used a rabbit anti-GFAP antibody (Dako, 1:500, catalogue number Z0334) and goat anti-rabbit secondary antibody, Alex Fluor 647 (1:500, catalogue number A-21245). Fluorescence images were examined with an Inverted Axio Observer 3 microscope (Carl Zeiss, Jena, Germany) equipped with an Axiocam 512 camera. The images in *LepR^b-EGFP* mice were acquired at a resolution of 2363 × 2544 pixels with an LD A-Plan 20×/0.35 Ph 1 objective and a resolution of 4248 × 2832 pixels with an LD A-Plan 40×/0.55 Ph 1 objective. The images in *db/db* mice photos were acquired at a resolution of 2179 × 2194 pixels with an LD A-Plan 20×/0.35 Ph 1 objective and a resolution of 4248 × 2832 pixels with an LD A-Plan

40×/0.55 Ph 1 objective. The following filters were used: for DAPI, the led module-385 nm filter; for Alexa 647 the led module-630 nm filter, for Alexa 568 the led module-567 nm filter, and for EGFP the led module-475 nm filter. All images were processed to merge with the software Carl Zeiss Image.

We quantified the number of glomus (type I) cells and type II cells and the proportion of cells expressing leptin receptor ($LepR^{b+}$ cells) from the immunohistochemistry images of CB of $LepR^b$ -EGFP mice and Ad - $LepR^b$ -infected db/db mice. Cells were manually counted from images taken under a 20× or 40× microscope objective. All measurements were performed by the same investigator using the count tool of the Adobe Photoshop CS5.1 (Adobe Systems) software. First, we counted the total number of type I and II cells in the CB, merging the pictures of DAPI with GFAP (Alexa 647) and TH (Alexa 568). Quantification of $LepR^b$ cells was performed by merging the pictures of EGFP staining with a type I (glomus) cell marker TH (Alexa 568) and a type II cell marker GFAP (Alexa 647).

Statistical analyses

All analyses were performed using STATA version 14.0 (StataCorp LLC, College Station, TX, USA) and prism 7.0 (GraphPad Software, La Jolla, CA, USA). We used the Wilcoxon matched-paired signed rank test, paired t test and Mann–Whitney U test to compare variables before and after specific treatments, and two-way ANOVA to examine interactions and the independent effect of two treatments. Mixed effects regression models were performed to investigate the independent effects of treatments with random intercepts to account for differences between mice. P values < 0.05 were considered statistically significant.

Results

Leptin increased baseline minute ventilation and HVR in C57BL/6J mice and leptin's effects were abolished by CSND

The cellular distribution of $LepR^b$ in mouse CB was first determined in $LepR^b$ -EGFP mice. Quantitative analysis of immunofluorescence images showed that TH⁺ type I cells represented $90.4 \pm 1.1\%$, whereas GFAP⁺ type II cells represented $9.6 \pm 1.3\%$ of the CB cellular population (Fig. 2A–C). The expression of $LepR^b$ in type I and type II CB cells was determined by EGFP fluorescence, which was present in $73.8 \pm 5.9\%$ of type I cells and $61.1 \pm 9.3\%$ of type II cells (Fig. 2). Of note, $LepR^b$ was not detected in the superior cervical ganglia (Fig. 2A).

The effect of leptin on CSN activity was assessed *in vivo* in anaesthetized mechanically ventilated mice

during 100% O₂ hyperoxia and 10% O₂ hypoxia. Leptin significantly increased CSN activity during hyperoxia and augmented CSN response to hypoxia (Fig. 3). In contrast, vehicle (saline) injections did not have an effect.

HVR measurements were performed in unrestrained unanaesthetized C57BL/6J mice during quiet wakefulness before and after CSND or sham surgery. CSND or sham CSND did not affect mouse body weight or food intake, whereas, as expected, leptin increased body temperature and suppressed food intake resulting in weight loss, regardless of the CSND status (Tables 2 and 3). There was no significant change in body temperature during HVR measurements. For example, in mice with intact CB rectal temperature was $35.8 \pm 0.1^\circ\text{C}$ and $35.7 \pm 0.1^\circ\text{C}$ immediately before and after the measurements, respectively.

Hypoxic exposure resulted in severe oxyhaemoglobin desaturation with S_{pO_2} declining from a median value of 98.6% at normoxic conditions to 71% during hypoxia (Fig. 1B). Prior to CSND, continuous infusion of leptin increased V_E from 1.1 to 1.5 mL/min/g during normoxia (20.9% O₂, $P < 0.01$ vs. saline infusion, Fig. 4A) and from 3.6 to 4.7 mL/min/g during isocapnic hypoxia (10% O₂ + 3% CO₂, $P < 0.001$, Fig. 5A). Leptin increased both respiratory rate, from 125 to 138 during normoxia ($P < 0.05$, Fig. 4B) and from 224 to 234 during hypoxia ($P < 0.05$, Fig. 5B), and tidal volume, from 0.009 to 0.011 mL/g during normoxia ($P < 0.05$, Fig. 4C) and from 0.015 to 0.020 mL/g during hypoxia ($P < 0.01$, Fig. 5C). Leptin increased the HVR, from 0.23 to 0.31 mL/min/g/ ΔF_{IO_2} ($P < 0.001$, Fig. 5D).

CSND had no effect on S_{pO_2} , P_{aO_2} or P_{CO_2} (Fig. 1C, Table 1), although there was a significant decline in the alveolar–arterial O₂ gradient at room air conditions, from 18.6 ± 4.8 mmHg before CSND to 0 ± 5.7 mmHg after CSND ($P < 0.05$), suggesting improvement in ventilation/perfusion matching. CB denervation did not affect V_E at normoxic conditions (Fig. 4). In contrast, CSND significantly decreased V_E and respiratory rate during hypoxic exposure and markedly attenuated the HVR (Fig. 5). CSND abolished the effects of leptin on minute ventilation during normoxia (Fig. 4A) and hypoxia (Fig. 5A) and abolished the leptin-induced increase in HVR (Fig. 5D). In contrast to CSND, sham surgery did not affect minute ventilation or HVR and did not attenuate the effect of leptin (Fig. 6).

$LepR^b$ expression in the CB of $LepR^b$ -deficient db/db mice increased baseline minute ventilation in awake and sleeping mice and increased the HVR

The cellular composition of the CB in db/db mice was similar to that in $LepR^b$ -EGFP mice; $86.5 \pm 1.5\%$ of all cells were TH⁺ type I cells and $13.5 \pm 1.5\%$ were GFAP⁺ type II cells (Fig. 7). Ad - $LepR^b$ infection of the CB sites resulted in

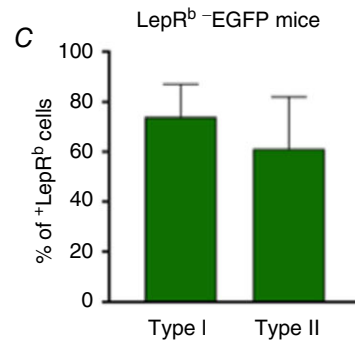
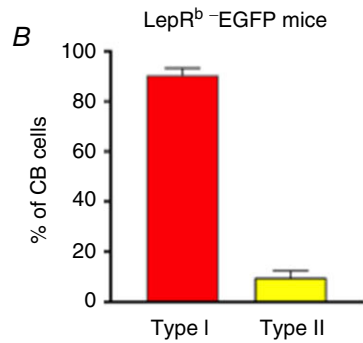
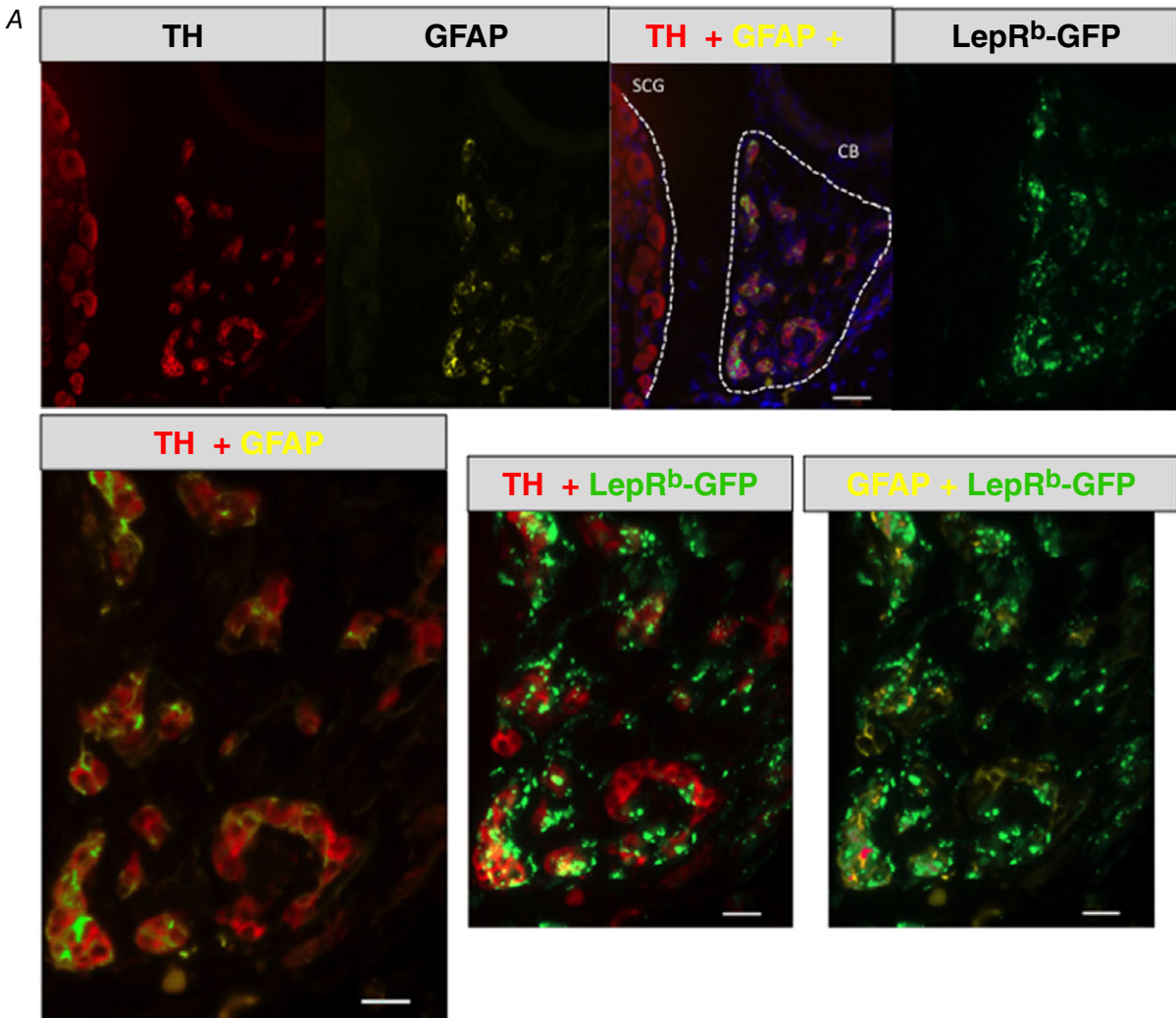


Figure 2. The long isoform of leptin receptor (LepR^b) was expressed in tyrosine hydroxylase (TH)-positive type I (glomus) cells and glial fibrillary acidic protein (GFAP)-positive type II cells of the carotid bodies of LepR^b-EGFP mice

A, co-localization of TH (red), GFAP (yellow) and LepR^b-EGFP (green) in the carotid bodies (CB) and superior cervical ganglion (SCG). Upper panel: 20 \times , scale bar = 20 μ m; lower panel, 40 \times , scale bar = 50 μ m. B, percentage of type I (TH-positive cells) and type II (GFAP-positive cells) cells in the carotid bodies. C, percentage of type I and type II cells expressing LepR^b ($n = 5$).

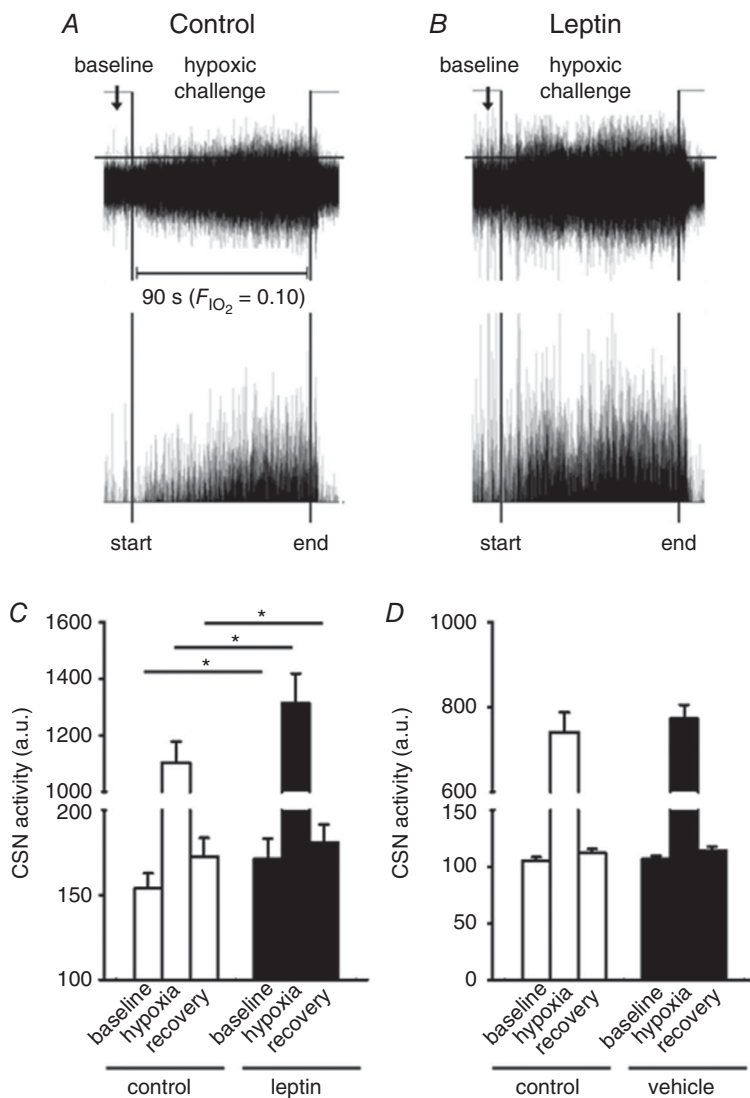
Table 2. Basic characteristics of C57BL/6J mice during saline and leptin infusion before and after carotid sinus nerve dissection

	Intact carotid bodies				Carotid sinus nerve dissection			
	Leptin infusion (n = 12)		Saline infusion (n = 12)		Leptin (n = 9)		Saline infusion (n = 9)	
	Baseline	48 h Leptin pump	Baseline	48 h Saline pump	Baseline	48 h Leptin pump	Baseline	48 h Saline pump
Body weight (g)	25.42 ± 0.7	24.13 ± 0.8***	25.31 ± 0.7	25.6 ± 0.7	25.9 ± 1.4	24.9 ± 1.1*	26.5 ± 0.7	27.1 ± 0.6
Body temperature (°C)	35.2 ± 0.1	36.6 ± 0.2***	35.5 ± 0.1	35.7 ± 0.1	35.5 ± 0.2	36.6 ± 0.2*	35.6 ± 0.2	35.6 ± 0.2
Food intake (g/day)	3 ± 0.1	1.35 ± 0.1**	3.2 ± 0.1	3.4 ± 0.06	3.7 ± 0.01	1.5 ± 0.8***	3.6 ± 0.04	3.2 ± 0.8
Leptin (ng/mL)	ND	34.9 ± 4.3	ND	1.2 ± 0.3†††	ND	36.1 ± 8.3	ND	1.5 ± 0.6††

* $P < 0.05$, ** $P < 0.01$, *** $P < 0.001$ for differences between baseline and leptin pump; †† $P < 0.01$ and ††† $P < 0.001$ for the difference between saline and leptin infusion. ND, not done. Results are presented as mean ± SEM.

abundant expression of the long isoform of leptin receptor ($LepR^b$), which was present in 100% of type I and type II cells (Fig. 7). Of note, $Ad-LepR^b$ infection was not specific to the CB, involving other adjacent tissues such as the superior cervical ganglion neurons (Fig. 7).

$LepR^b$ expression in the CB did not affect food intake, rectal temperature or body weight and there was no difference in circulating leptin levels between $Ad-LepR^b$ - and $Ad-LacZ$ -treated db/db mice (Table 4). As expected (Handa *et al.* 2014), circulating leptin levels in db/db mice

**Figure 3. Leptin augmented the carotid sinus nerve (CSN) response to hypoxia *in vivo***

CSN was dissected in a sedated, tracheostomized and mechanically ventilated C57BL/6J mouse subject to neuromuscular blockade, which was exposed to 100% O₂ (hyperoxia) followed by 10% O₂ hypoxia before and after intravenous infusion of leptin (0.3 μg). Representative tracings of the CSN recordings before and after leptin infusions are shown in the upper panels of A and B, respectively. For clarity, the lower panels are plotted to show activities above the user-defined threshold (horizontal lines). C, mean total CSN activity recorded before (baseline), during (hypoxia) and after (recovery) the hypoxic challenges in mice before and after leptin infusions (n = 10, * $P < 0.05$); D, mean total CSN activity recorded before and after vehicle (saline) infusions (n = 8).

Table 3. Basic characteristics of C57BL/6J mice during saline and leptin infusion before and after sham surgery

	Intact carotid bodies				Sham carotid sinus nerve dissection			
	Leptin infusion (n = 5)		Saline infusion (n = 5)		Leptin (n = 5)		Saline infusion (n = 5)	
	Baseline	48 h Leptin pump	Baseline	48 h Saline pump	Baseline	48 h Leptin pump	Baseline	48 h Saline pump
Body weight (g)	23.2 ± 0.8	21.7 ± 0.8***	22.5 ± 0.6	22.5 ± 0.6	24.6 ± 0.7	20.8 ± 0.4*	23.2 ± 0.5	23.1 ± 0.5
Body temperature (°C)	35.9 ± 0.3	37.5 ± 0.3**	35.5 ± 0.1	35.9 ± 0.3	35.8 ± 0.2	37.2 ± 0.07*	35.4 ± 0.1	35.7 ± 0.1
Food intake (g/day)	3.9 ± 0.0	0.78 ± 0.03***	3.5 ± 0.18	3.2 ± 0.2	3.7 ± 0.15	0.9 ± 0.1***	4.6 ± 0.15	4.15 ± 0.15
Leptin (ng/mL)	ND	73.8 ± 30.2††	ND	1.1 ± 0.5	ND	143 ± 16.4††	ND	1.1 ± 0.6

* $P < 0.05$, ** $P < 0.01$, *** $P < 0.001$ for differences between baseline and leptin pump; †† $P < 0.01$ for the difference between saline and leptin infusion. ND, not done. Results are presented as mean ± SEM.

Table 4. Basic characteristics of *Ad-LepR^b* and *Ad-LacZ* infected *db/db* mice

	Ad-LacZ		Ad-LepR ^b	
	Baseline	After infection	Baseline	After infection
Sample number (N)	11	11	14	14
Body weight (g)	51.0 ± 1.9	54.7 ± 2.9	50.3 ± 1.7	52.4 ± 1.7
Body temperature (°C)	34.6 ± 0.2	34.7 ± 0.3	34.4 ± 0.2	34.5 ± 0.3
Food intake (g/day)	5.5 ± 0.5	5.5 ± 1.1	5.2 ± 0.2	5.2 ± 0.2
Leptin (ng/mL)	ND	62.1 ± 3.24	ND	57.2 ± 5.9

ND, not done. Results are presented as mean ± SEM.

were similar to those in C57BL/6J mice during infusion of leptin (compare Tables 2 and 4).

V_E was measured in *db/db* mice during quiet wakefulness before and 15 days after *Ad-LepR^b* or *Ad-LacZ* infections. Hypoxic exposure resulted in severe oxyhaemoglobin desaturations with median S_{pO_2} decreasing from 98.8% to 63% and there was no significant effect of *Ad-LepR^b* (Fig. 1D and E). *LepR^b* expression in the CB increased minute ventilation from 1.1 to 1.3 mL/min/g during normoxia ($P < 0.05$, Fig. 8A) and from 2.8 to 3.2 mL/min/g during hypoxia ($P < 0.05$, Fig. 9A). The expression of the long isoform of leptin receptor increased tidal volumes (Figs. 8E and 9E), while respiratory rate was not significantly changed (Figs. 8C and 9C). *LepR^b* expression consistently increased the HVR when quantified with either ΔF_{IO_2} or ΔS_{pO_2} ($P < 0.05$, Fig. 10A and C). Control *Ad-LacZ* infection did not affect any of the respiratory parameters (Figs. 8–10). Short hypoxic exposures during HVR measurements did not significantly decrease body temperature.

Sleep recordings showed that *LepR^b* expression in the CB decreased the amount of NREM sleep in *db/db* mice compared to *LacZ* control, whereas other sleep metrics (sleep efficiency, amount of REM sleep, number and length of sleep bouts) were unaffected (Table 5). Expression of *LepR^b* in the CB of *db/db* mice did not influence the prevalence of upper airway obstruction. In *Ad-LepR^b*-infected mice, the percentage of breaths with inspiratory flow limitation was $0.1 \pm 0.1\%$ in NREM

sleep and $23 \pm 6\%$ in REM sleep, whereas in *Ad-LacZ* mice, inspiratory flow limitation was observed in $2 \pm 2\%$ and $25 \pm 11\%$ of breaths, respectively. However, *LepR^b* expression significantly increased minute ventilation, maximal and mean inspiratory flow and tidal volume compared to control (Figs. 11 and 12). Specifically, in *LepR^b* mice minute ventilation in NREM sleep was 27.7 mL/min vs. 20.1 mL/min in control ($P < 0.05$) and in REM sleep it was 23.4 mL/min vs. 16.5 mL/min in control ($P < 0.05$) (Fig. 12A). In *LepR^b* mice, mean inspiratory flow in NREM sleep was 1.3 mL/s vs. 0.9 mL/s in control ($P < 0.05$), and in REM sleep it was 1.0 mL/s vs. 0.7 mL/s in control ($P < 0.05$) (Fig. 12B). Maximal inspiratory flow in NREM sleep was 2.35 mL/s vs. 1.6 mL/s in control ($P < 0.05$), and in REM sleep it was 1.6 mL/s vs. 1.2 mL/s in control ($P < 0.05$) (Fig. 12C). *LepR^b* expression increased tidal volumes (Fig. 12D) but not respiratory rate (Fig. 12E). There was no significant effect of leptin on the ODI (Fig. 12F). Sigh frequency varied greatly between mice. In the *Ad-LepR^b* group it fluctuated from 0 to 15.1/h, with a median of 7.4/h, whereas in the *Ad-LacZ* group it varied from 0 to 8.5/h, with a median of 4.3/h; there was no difference in sigh frequency between the groups ($P > 0.05$).

Discussion

The main novel finding of our study was that leptin acted in the CB to increase minute ventilation at normoxic conditions in awake and sleeping mice. This finding

was confirmed by several independent lines of evidence. First, leptin increased minute ventilation at normoxic conditions in awake C57BL/6J mice and this increase was abolished by CB denervation, but not by sham surgery. Second, expression of the long isoform of leptin receptor *LepR^b* in the CB increased minute ventilation at normoxic conditions in awake and sleeping *LepR^b*-deficient *dbl/db* mice. Third, intravenous infusion of leptin increased CSN activity *in vivo* at hyperoxic conditions, when CB activity is suppressed (Ling *et al.* 1997). In addition, we report several other important findings. We have shown that leptin acts in the CB to augment the HVR in C56BL/6J mice and this effect was abolished by CB denervation, similar to a recent report in rats (Yuan *et al.* 2018). Parallel experiments in *dbl/db* mice confirmed that this effect is

mediated by the *LepR^b* receptor. Finally, we are first to report on the quantitative morphometry of *LepR^b* in the CB, showing its ubiquitous distribution in both type I and type II cells.

Leptin's effect on CB and respiratory function during normoxia

We have shown that leptin infusion increases baseline ventilation in C57BL/6J mice. The stimulating impact of leptin on minute ventilation was described two decades ago in *ob/ob* mice (O'Donnell *et al.* 1999). Leptin's action can be attributed in part to an increase in metabolic rate and CO₂ production with ensuing increases in minute ventilation (Gautron & Elmquist, 2011). However, leptin

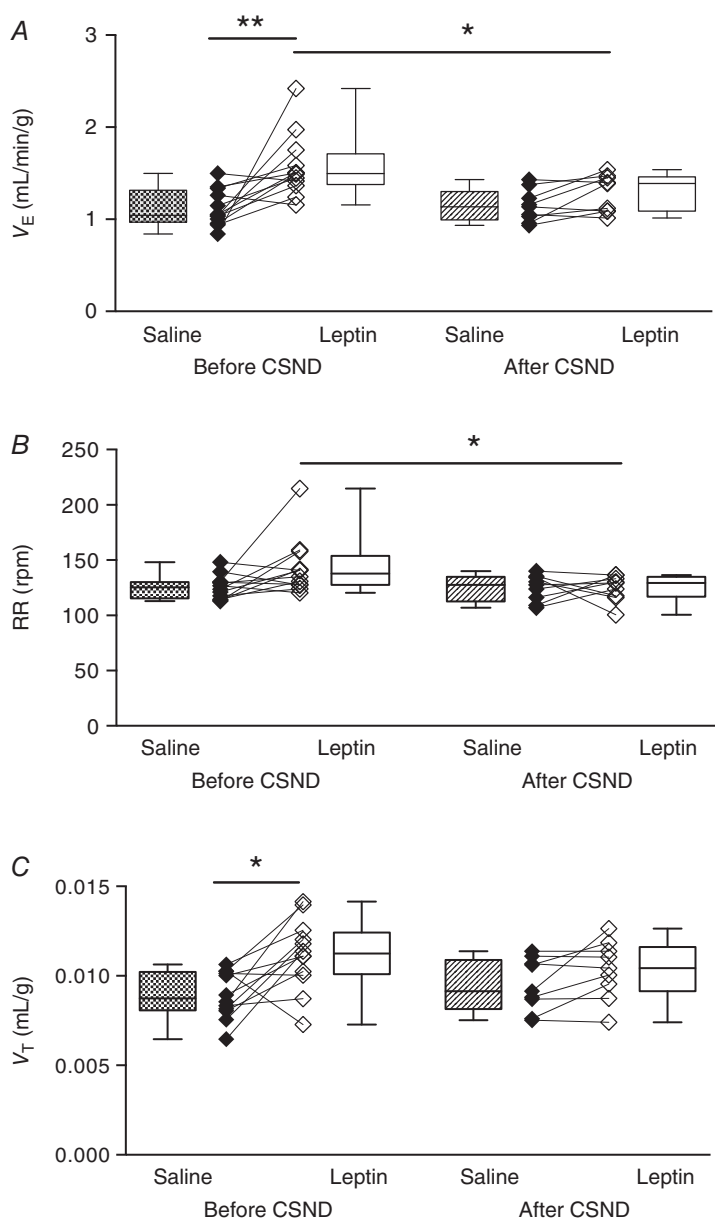


Figure 4. Leptin augmented minute ventilation (V_E) at normoxic conditions (21% O₂) and this effect was abolished by carotid sinus nerve dissection (CSND) in C57BL/6J mice during quiet wakefulness

A, V_E was calculated as tidal volume per body weight (V_T) \times respiratory rate (RR) at 21% O₂ during saline and leptin continuous infusions (120 μ g/day, s.c.) measured before ($n = 12$) and after ($n = 9$) CSND. B and C, RR (B) and V_T (C) values at the same conditions. * $P < 0.05$, ** $P < 0.01$ using the Wilcoxon test for paired comparisons and Mann–Whitney test for unpaired comparisons.

also acts as a respiratory stimulant, independent of its metabolic effects (O'Donnell *et al.* 1999). Leptin-deficient *ob/ob* mice show a suppressed minute ventilation and hypercapnic ventilatory response, which are normalized by leptin infusion (O'Donnell *et al.* 1999). Leptin

infusion did not increase minute ventilation in lean Zucker rats, but the investigators induced a very modest increase in circulating leptin level (1.6-fold from baseline, Yuan *et al.* 2018), whereas we induced an ~ 30-fold increase in leptin, similar to that observed in obese mice

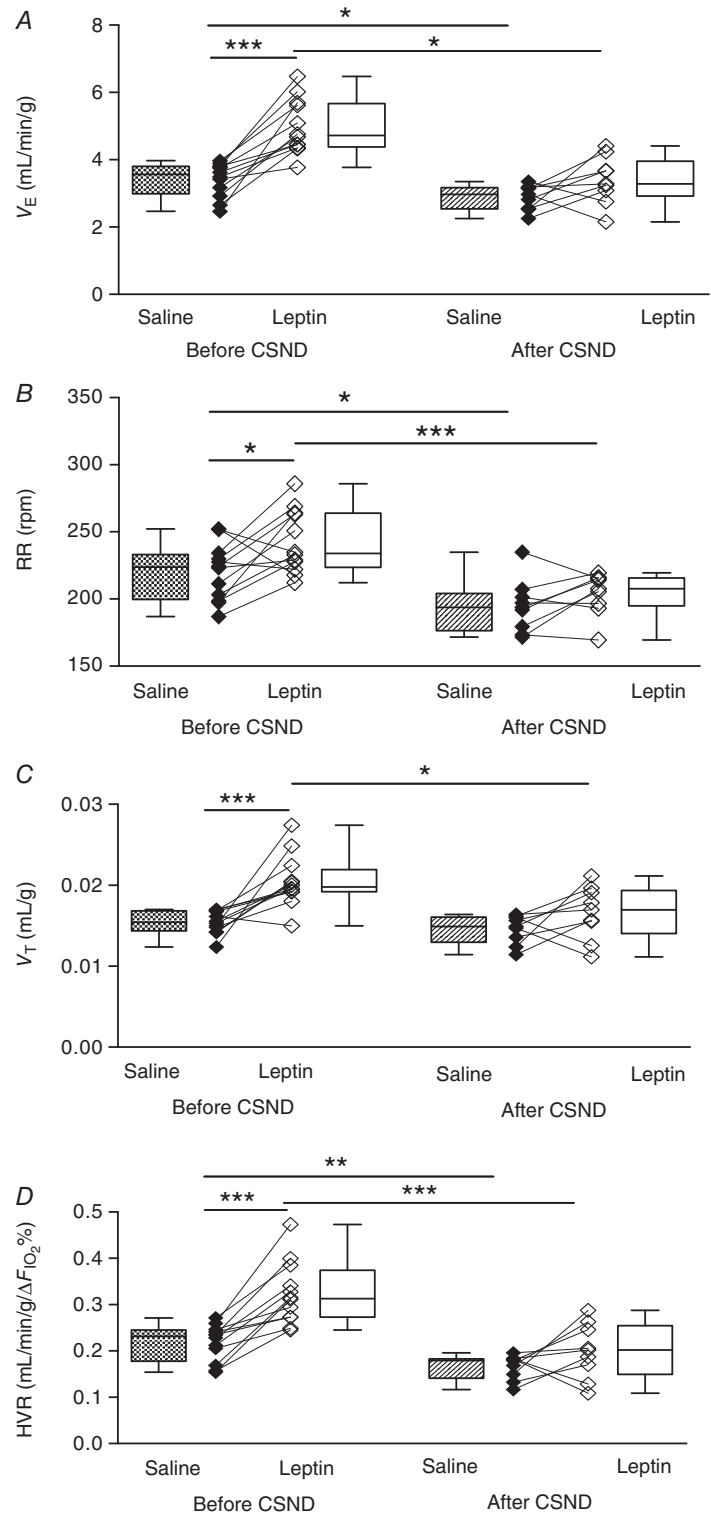


Figure 5. Leptin augmented minute ventilation (V_E) at isocapnic hypoxia (10% O_2 + 3% CO_2) and the hypoxic ventilatory response (HVR) and the effects were abolished by carotid sinus nerve dissection (CSND) in C57BL/6J mice during quiet wakefulness

A, V_E was calculated as tidal volume per body weight (V_T) \times respiratory rate (RR) at 10% O_2 during saline and leptin continuous infusion (120 μ g/day, *s.c.*) measured before ($n = 12$) and after ($n = 9$) CSND. B and C, RR (B) and V_T (C) values at the same conditions. D, HVR represents the ratio of a change in V_E to a change in the fraction of inspired oxygen ($HVR = \Delta V_E / \Delta F_{IO_2}$) at the conditions described above. * $P < 0.05$, ** $P < 0.01$, *** $P < 0.001$ using the Wilcoxon test for paired comparisons and Mann–Whitney test for unpaired comparisons.

(Fleury Curado *et al.* 2018) and humans (Phipps *et al.* 2002; Shapiro *et al.* 2014). Intracerebroventricular administration of leptin instantaneously increased respiration in *ob/ob* mice (Bassi *et al.* 2012; Yao *et al.* 2016), whereas microinjections of leptin into the retrotrapezoid nucleus/parafacial respiratory group in *ob/ob* mice (Bassi *et al.* 2014) and into the NTS in rats (Inyushkina *et al.* 2010) localized respiratory effects of leptin to CO₂ sensing areas. Thus, leptin is a potent respiratory stimulant acting on respiratory control centres in the medulla.

What evidence is there that leptin regulates breathing at normoxic conditions via peripheral chemoreception?

LepR^b, the only *LepR* isoform capable of intracellular signalling, has been previously identified in the CB of rats (Porzionato *et al.* 2011; Messenger *et al.* 2013; Messenger & Ciriello, 2013). We report that *LepR^b* was present in > 70% of the CB glomus cells and > 60% of type II cells. Intracarotid administration of leptin increased minute ventilation in anaesthetized rats (Ribeiro *et al.* 2018). Leptin increased baseline CSN activity *in vitro* (Ribeiro *et al.* 2018) and *in vivo* according to our current data. We have shown that leptin increased minute ventilation in awake unrestrained C57BL/6J mice at normoxic conditions and its effect was abolished by CB denervation.

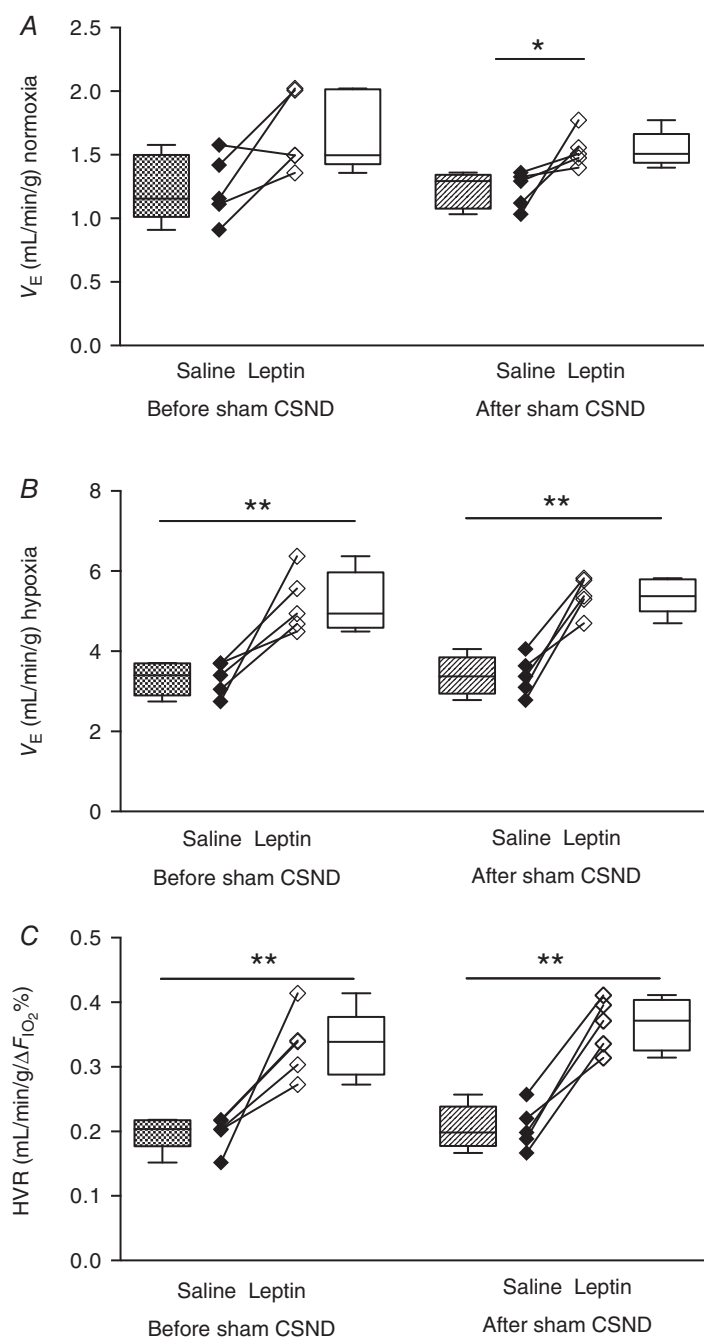


Figure 6. Leptin augmented minute ventilation (V_E) and the hypoxic ventilatory response (HVR) and this effect was not modified by sham carotid sinus nerve dissection (CSND) in C57BL/6J mice during quiet wakefulness

A and B, V_E was calculated as tidal volume per body weight (V_T) \times respiratory rate (RR) at 21% O₂ (A) and 10% O₂ (B) during saline and leptin continuous infusion (120 μ g/day, s.c.) measured before ($n = 5$) and after ($n = 5$) sham CSND. C, HVR represents the ratio of a change in V_E to a change in the fraction of inspired oxygen ($HVR = \Delta V_E / \Delta F_{IO_2}$). * $P < 0.05$, ** $P < 0.01$ using the Mann–Whitney test for unpaired comparisons.

LepR^b expression in the CB of hyperleptinaemic *db/db* mice also increased minute ventilation, during both sleep and wakefulness. We provide two independent lines of evidence that leptin regulates respiratory function in the CB, independent of its metabolic effects. First, in C57BL/6J mice, leptin infusion suppressed food intake and increased metabolic rate and these effects were not attenuated by CSND (Table 2), whereas leptin-induced

augmentation of minute ventilation was abolished by CB denervation. Second, *LepR^b* expression in the CB of *LepR^b*-deficient *db/db* mice did not affect food intake or body temperature (Table 4), whereas minute ventilation was increased, during both wakefulness and sleep (Figs. 8 and 12). Our data suggest that leptin's action in the CB plays an important role in the CB afferent input to the brainstem respiratory centres. Thus, our study provides

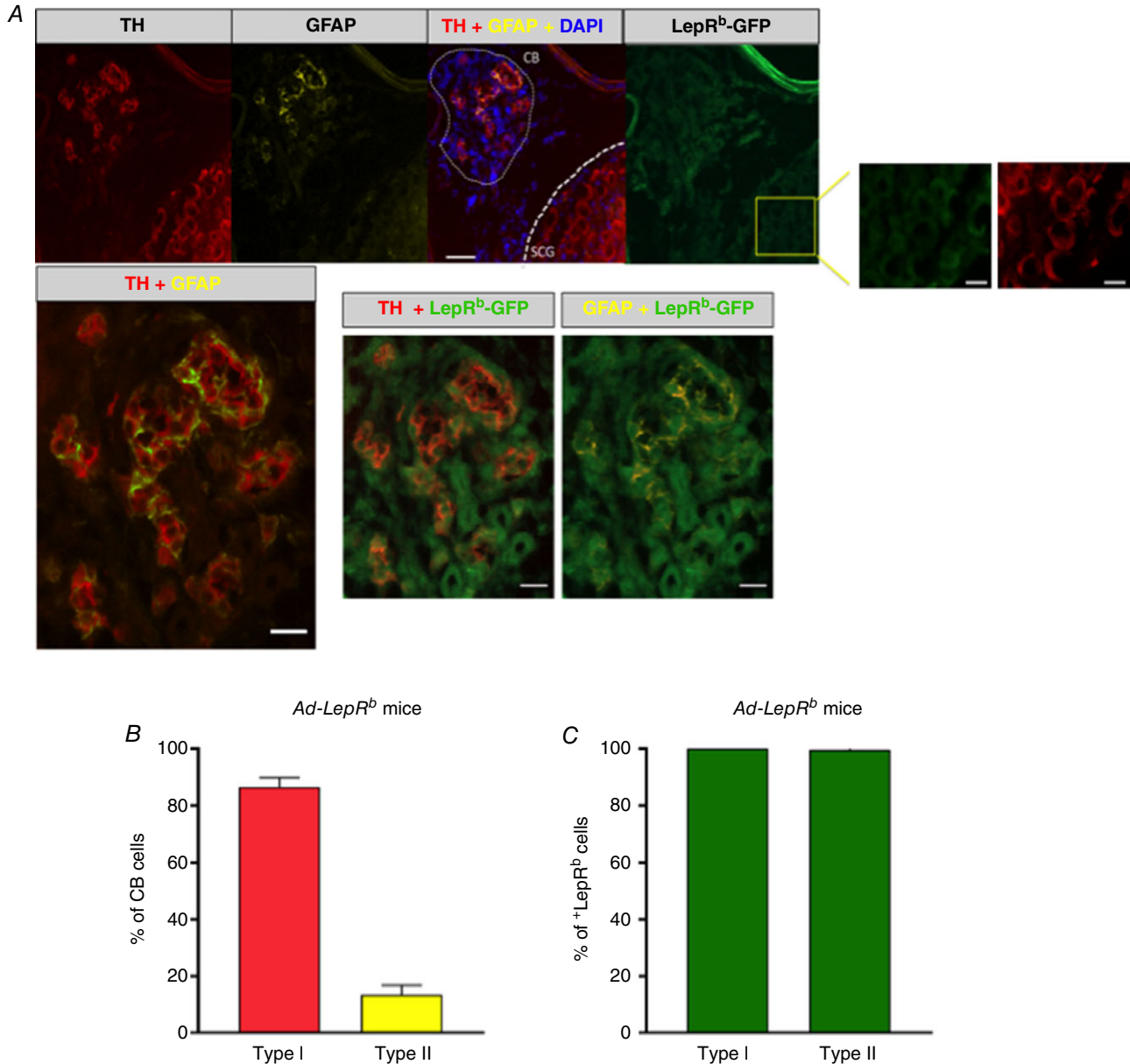


Figure 7. The long functional isoform of leptin receptor (*LepR^b*) was expressed in tyrosine hydroxylase (TH)-positive type I (glomus) cells and glial fibrillary acidic protein (GFAP)-positive type II cells of the carotid body of *LepR^b*-deficient obese *db/db* mice after *Ad-LepR^b*-GFP infection

A, co-localization of TH (red), GFAP (yellow) and *LepR^b*-GFP (green) in the carotid bodies (CB) and superior cervical ganglion (SCG). The enlarged insert on the right shows *LepR^b*-GFP-TH-positive cells in SCG. Upper panel: 20×, scale bar = 50 μm, scale bar for the inserts is 20 μm; lower panel: 40×, scale bar = 20 μm. B, percentage of type I (TH-positive) cells and type II (GFAP-positive) cells in the carotid bodies. C, percentage of type I and type II cells expressing *LepR^b* (n = 5).

first evidence that leptin acts in the CB to augment minute ventilation at normoxic conditions in unanaesthetized awake and sleeping mice.

Leptin's effect on CB and the HVR

The effect of leptin on the hypercapnic ventilatory response is well recognized (Tankersley *et al.* 1996; O'Donnell *et al.* 1999; Polotsky *et al.* 2001, 2004;

Bassi *et al.* 2014). In contrast, the role of leptin in regulation of the HVR has not been convincingly defined. Tankersley *et al.* (1996) studied young leptin-deficient *ob/ob* mice, mice heterozygous for the leptin gene and weight-matched wild-type mice and found similar HVR in all groups. However, leptin was not administered and leptin-deficient mice were not compared to mice with severe diet-induced obesity with very high circulating leptin levels. Our data provide first evidence in mice

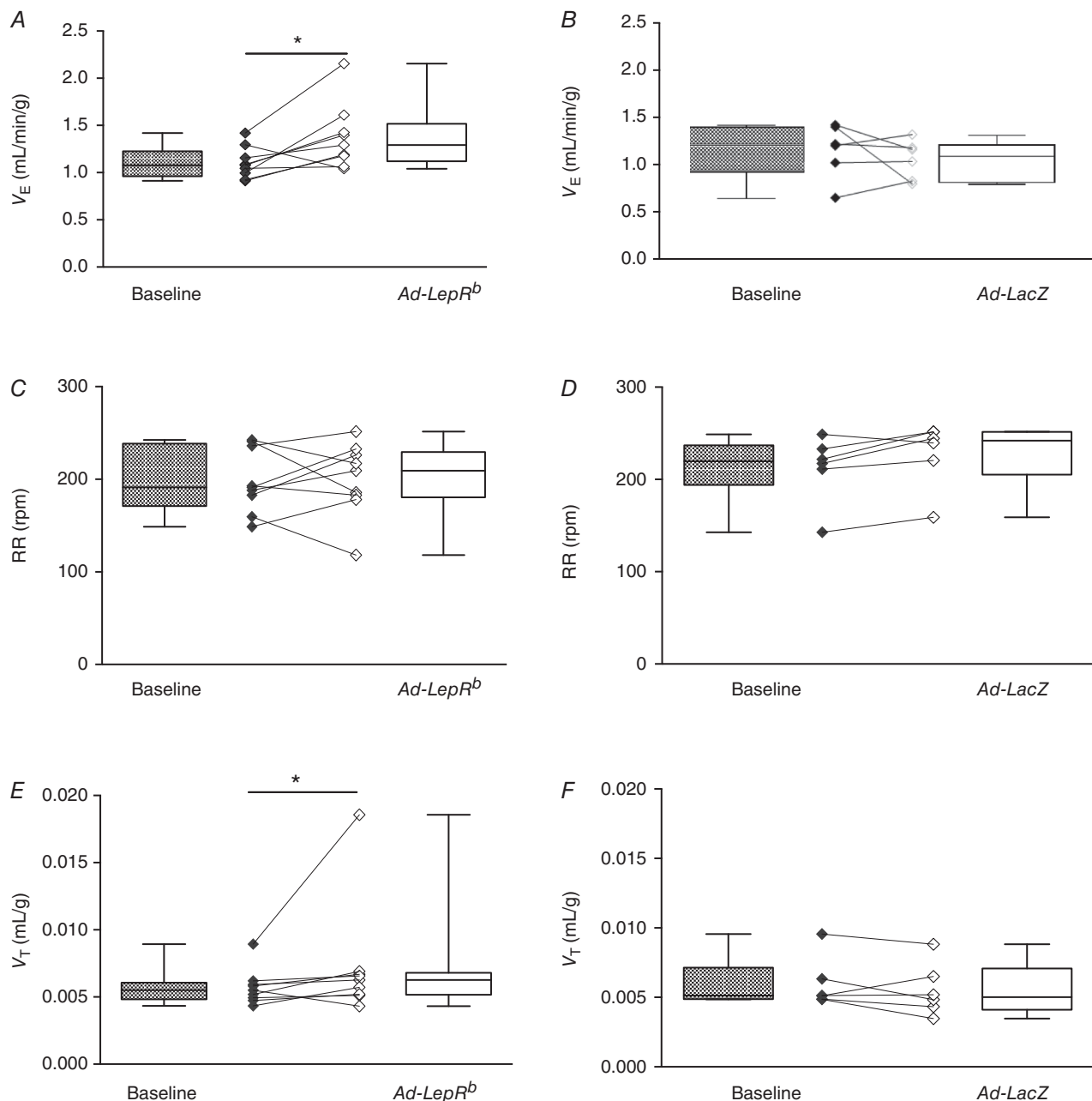


Figure 8. *LepR^b* expression in the carotid bodies (CB) of *LepR^b*-deficient *db/db* mice increased minute ventilation (V_E) at normoxic conditions (21% O_2)

A and B, V_E calculated as tidal volume per body weight (V_T) \times respiratory rate (RR), RR (C and D) and V_T (E and F) before (baseline) and 15 days after *Ad-LepR^b* ($n = 9$) or *Ad-LacZ* ($n = 6$) infection, at the same conditions.

* $P < 0.05$ using the Wilcoxon test.

that leptin augments CSN activity in response to physiologically relevant levels of hypoxia *in vivo* and confirm previous findings in rats (Yuan *et al.* 2018) that leptin increases the HVR in awake unrestrained spontaneously breathing rodents. The HVR varied significantly between mice in each group, which is not surprising given that HVR measurements are typically variable within a subject (Teppema & Dahan, 2010). Nevertheless, our study overcame this intrinsic variability using within-animal

comparisons (before and after CSND, before and after *Ad-LepR^b* transfection) and appropriate controls (sham surgery and *Ad-LacZ* transfection). Our findings are consistent with previously published data that leptin induced CSN activity in response to anoxia in the *ex vivo* preparations (Shirahata *et al.* 2015; Ribeiro *et al.* 2018) and augmented ventilation in anaesthetized tracheostomized rats during bilateral carotid artery occlusion (Ribeiro *et al.* 2018).

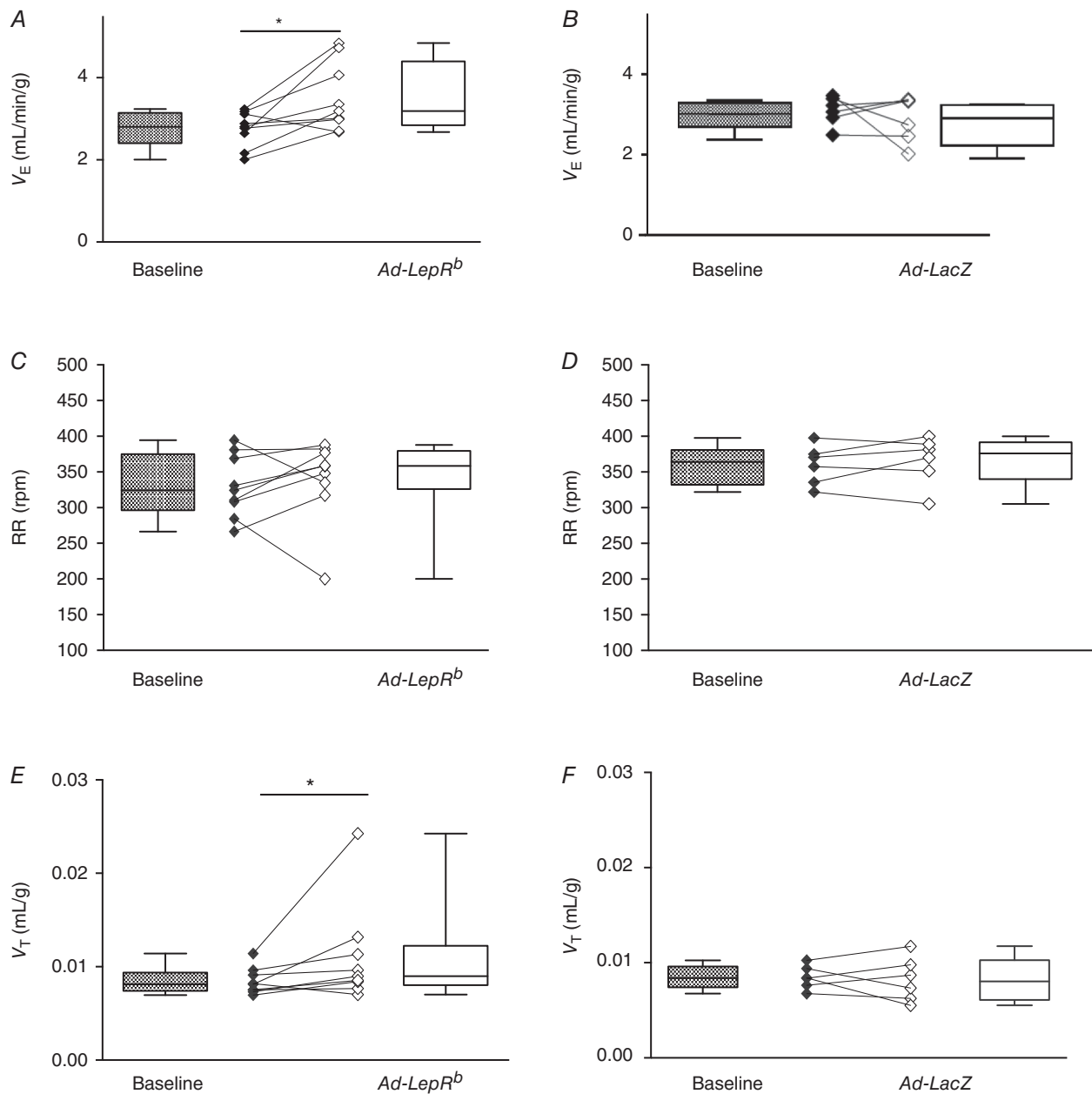


Figure 9. *LepR^b* expression in the carotid bodies (CB) of *LepR^b*-deficient *db/db* mice increased minute ventilation at isocapnic hypoxia (10% O_2 + 3% CO_2)

A and B, V_E calculated as tidal volume per body weight (V_T) \times respiratory rate (RR). RR (C and D) and V_T (E and F) before (baseline) and 15 days after *Ad-LepR^b* ($n = 9$) or *Ad-LacZ* ($n = 6$) infection, at the same conditions. * $P < 0.05$ and ** $P < 0.01$ using the Wilcoxon test.

Table 5. Sleep architecture in *db/db* mice after *Ad-LacZ* and *Ad-LepR* infection of the carotid bodies

	Sleep efficiency (% of total time)	Sleep bouts						
		Sleep duration (min)			Sleep bouts			
		Total	NREM	REM	Number		Length (min)	
				NREM	REM	NREM	REM	
<i>Ad-LacZ</i>	54.40 ± 0.05	215.4 ± 26	208 ± 27	7.51 ± 4.0	107.8 ± 10.7	6 ± 3.2	1.8 ± 0.3	1.02 ± 0.3
<i>Ad-LepR</i>	42.40 ± 0.05	146.6 ± 24	139.2 ± 23*	7.46 ± 1.07	80.8 ± 8.2	6.2 ± 1.6	1.6 ± 0.3	1.4 ± 0.2

* $P < 0.05$ vs. *Ad-LacZ*. Results are presented as mean ± SEM. NREM, non-rapid eye movement sleep; REM, rapid eye movement sleep.

The current study has demonstrated the importance of leptin receptor in the CB for control of breathing in three complementary experiments. First, in awake wild-type mice with ubiquitously expressed *LepR^b*, leptin dramatically augmented minute ventilation in the 10% O₂ environment and the HVR and both effects were abolished by CB denervation. Second, selective expression of *LepR^b* in the CB of *LepR^b*-deficient *db/db* mice significantly enhanced minute ventilation at hypoxic conditions and augmented the HVR. Third, *db/db* mice transfected with *LepR^b* in the CB showed significant increases in both maximal and mean inspiratory flow during NREM and REM sleep, which suggests that leptin signalling in the CB

stimulates the respiratory drive (O'Donnell *et al.* 1999; Pho *et al.* 2016). Thus, the leptin-dependent mechanism in the CB stimulates the hypoxic ventilatory response and regulates respiratory drive during sleep.

Clinical implications

Although breathing during sleep in leptin-resistant *db/db* mice has not been sufficiently studied, phenotypically similar leptin-deficient *ob/ob* mice exhibit both hypoventilation during sleep (O'Donnell *et al.* 1999) and obstructive sleep apnoea (Pho *et al.* 2016; Yao *et al.* 2016), which can be treated with leptin. Our current

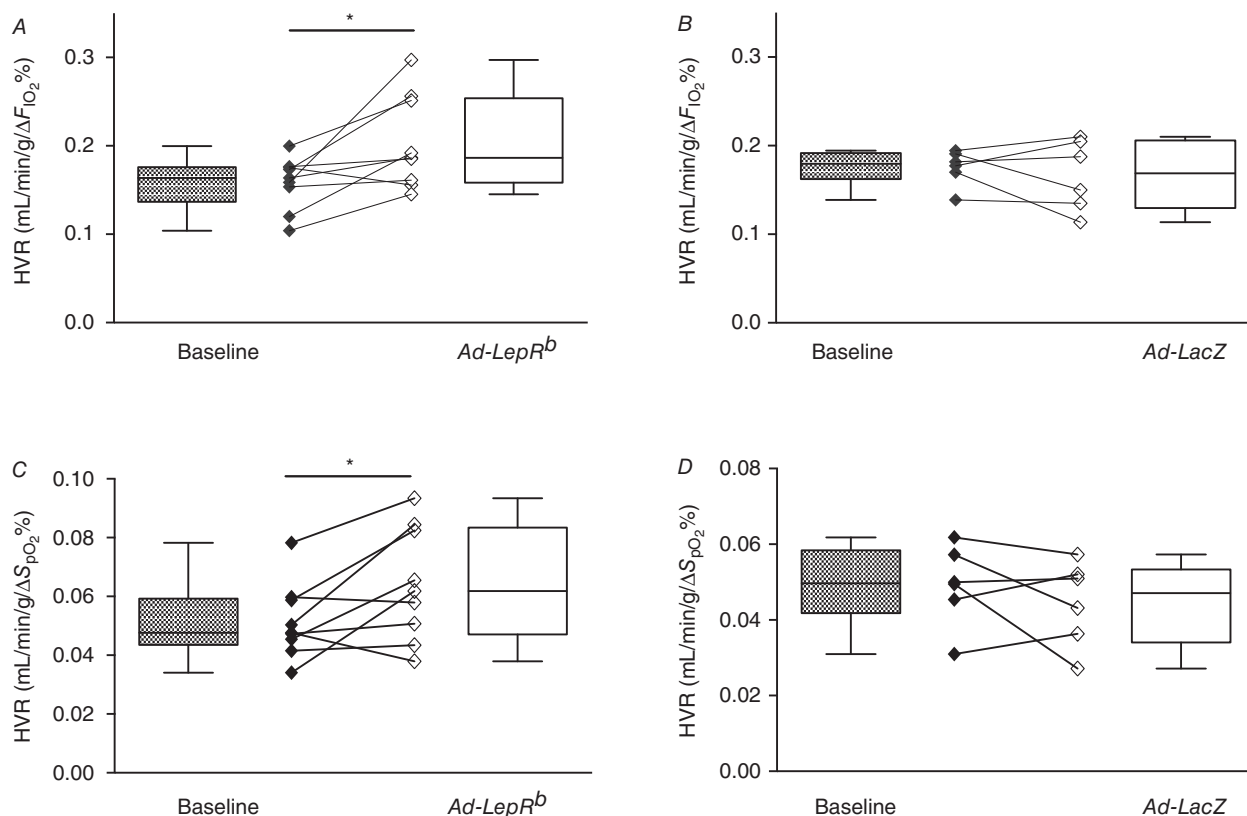


Figure 10. *LepR^b* expression in the carotid bodies (CB) of *LepR^b*-deficient *db/db* mice increased the hypoxic ventilatory response (HVR)

HVR calculated as $\Delta V_E/\Delta F_{IO_2}$ (A and B) and as $\Delta V_E/\Delta S_{pO_2}$ (C and D) before (baseline) and 15 days after *Ad-LepR^b* (A and C, $n = 9$) or *Ad-LacZ* (B and D, $n = 6$) infection. * $P < 0.05$ and ** $P < 0.01$ using the Wilcoxon test.

data showed that a leptin-dependent mechanism in the CB stimulates minute ventilation throughout NREM and REM sleep without any effect on upper airway obstruction, i.e. obstructive sleep apnoea. It is conceivable that leptin signalling in the CB protects the respiratory

function in severe obesity, preventing the development of obesity hypoventilation syndrome. Leptin may also play a role in maintaining oxygenation at the range of hypoxic conditions, including exposure to high altitude and hypoxaemia due to cardiorespiratory disorders.

Pathologically augmented HVR may destabilize breathing leading to central apnoea and aggravating obstructive apnoea (Younes *et al.* 2007; Pialoux *et al.* 2009; Trombetta *et al.* 2013; Younes, 2014; Mateika, 2015). According to our sleep data, leptin's action in the CB did not lead to apnoea, probably because mice were not hypoxaemic in the absence of exposure to hypoxic. Nevertheless, leptin-induced hypoxic hyperventilation during sleep may destabilize breathing by decreasing CO₂ below the apnoea threshold. Thus, leptin's action in the CB during sleep in the absence of significant hypoxaemia may be protective, whereas in the presence of hypoxaemia it may be destabilizing. In addition, leptin's action on the CSN may activate the sympathetic nervous system leading to a variety of poor outcomes including insomnia (note a decrease in NREM sleep time in Table 5) and cardiovascular complications (Prabhakar *et al.* 2012).

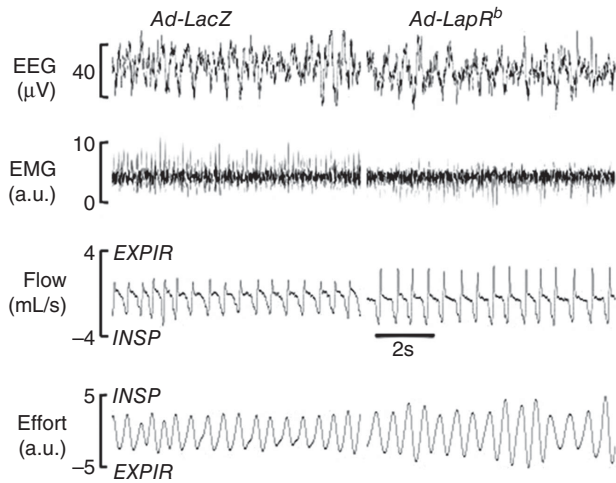


Figure 11. A representative recording of non-rapid eye movement sleep 15 days after infection of the carotid bodies with control virus (left, *Ad-LacZ*, *n* = 6) or after *LepR^b* expression in the carotid bodies of *db/db* mice *Ad-LepR^b* infection shows increased minute ventilation compared to the *Ad-LacZ* control. EEG, electroencephalography; EMG, electromyography of nuchal muscles; EXPIR, expiration; INSPIR, inspiration.

Limitations

Our study had potential limitations. (1) Hypoxia decreases \dot{V}_{O_2} and body temperature, which could affect respiratory measurements and their interpretations. Additionally, some animals had low rectal temperature at baseline, which could also affect measurements. However, short

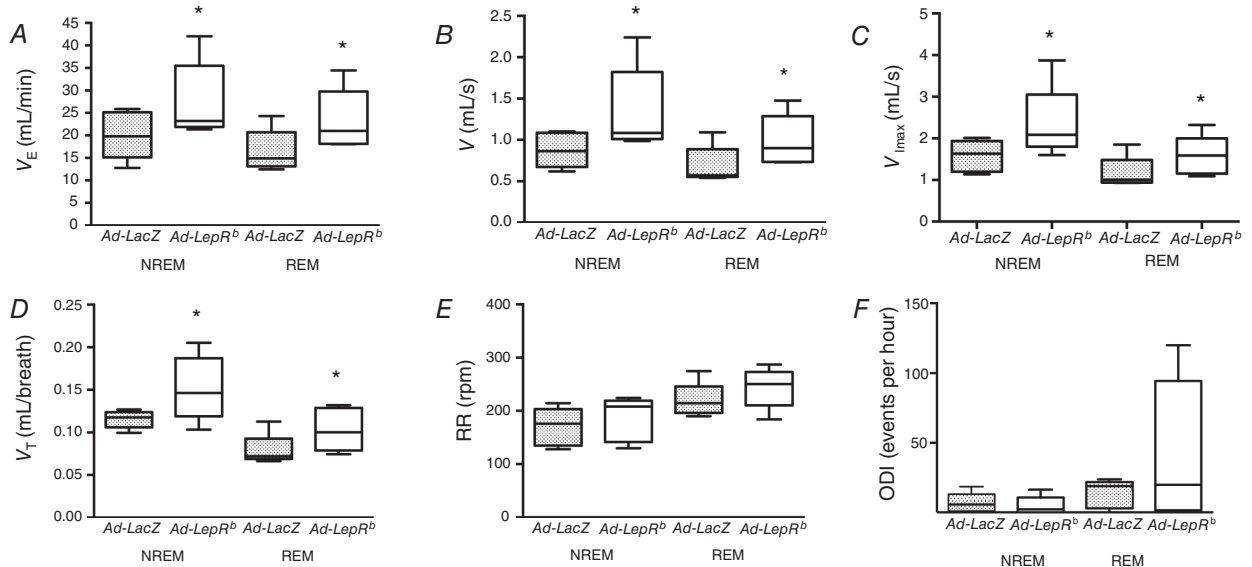


Figure 12. *LepR^b* expression in the carotid bodies of *LepR^b*-deficient *db/db* mice increased minute ventilation
 V_E (A), mean inspiratory flow rate (V , B), maximal inspiratory flow rate (V_{Imax} , C), and tidal volumes (V_T , D) during non-rapid eye movement (NREM) and rapid eye movement (REM) sleep, but not respiratory rate (RR, E), or oxygen desaturation index (ODI, F). *Ad-LepR* infected mice. * $P < 0.05$ shows the independent effect of *LepR^b* compared to the *Ad-LacZ* control by ANOVA.

exposures to hypoxia during HVR measurements did not decrease rectal temperature in our experiments. Hence, metabolic changes induced by hypoxia were unlikely to have an impact on ventilatory measurements during first 2 min of the hypoxic exposure. (2) We did not measure S_{pO_2} and arterial blood gas during leptin infusion due to technical limitations. (3) CSND did not affect P_{aO_2} , S_{pO_2} or P_{aCO_2} , despite a lack of an appropriate ventilatory response to hypoxia. This phenomenon could be attributed, at least in part, to improved ventilation/perfusion match in the lungs as indicated by a decrease in the alveolar–arterial O_2 gradient, probably as a result of a decrease in sympathetic vasoconstriction. (4) We did not examine downstream mechanisms by which leptin acts in the CB. Given that *LepR^b* is abundantly expressed in both oxygen sensing type I and type II cells, leptin's effect may occur in either cell type. In fact, Ribeiro *et al.* (2018) showed that leptin does not affect intracellular Ca^{2+} in type I cells *in vitro*, which questions the role of oxygen sensing glomus cells. Nevertheless, leptin's effects can differ between *in vitro* and *in vivo* conditions. Leptin may have chronic transcriptional effects mediated via Janus kinase 2/signal transducers and the activator of transcription 3 pathway or the phosphoinositide 3-kinase pathway (Villanueva & Myers, 2008). Leptin can stabilize hypoxia inducible factor 1 α (Calgani *et al.* 2016) in the glomus cells, which would enhance the HVR (Peng *et al.* 2006; Prabhakar & Semenza, 2012). Ribeiro *et al.* (2018) showed that leptin mediates adenosine release in the whole CB *ex vivo* preparation. Leptin may also act acutely to affect specific ion channels (Shirahata *et al.* 2015). Yuan *et al.* (2018) recently demonstrated that the effect of leptin on chemoreception may be mediated by oxygen sensing TASK channels. (5) *Ad-LepR^b* infection was not cell-specific, affecting both type I and type II cells of the CB as well as adjacent tissues such as the superior cervical ganglion. While the non-selective transfection technique is a limitation of the study, together with leptin studies in wild-type mice with denervated and intact (sham surgery) CB, and with CSN recordings *in vivo* in the absence and presence of leptin, our study provides evidence that leptin acts in the CB to regulate HVR. (6) We did not investigate whether the effects of leptin in the CB are modified by the leptin-resistant state such as diet-induced obesity (Ribeiro *et al.* 2018) or sexual differences (Polotsky *et al.* 2001). (7) We did not measure the HVR during sleep and did not determine whether leptin signalling in the CB in the presence of hypoxia has a destabilizing effect on breathing during sleep.

Conclusions

Leptin acts in the CB to augment minute ventilation and the hypoxic ventilatory response, which may protect against SDB in obesity.

References

- Bassi M, Furuya WI, Menani JV, Colombari DS, do Carmo JM, da Silva AA, Hall JE, Moreira TS, Wenker IC, Mulkey DK & Colombari E (2014). Leptin into the ventrolateral medulla facilitates chemorespiratory response in leptin-deficient (ob/ob) mice. *Acta Physiol (Oxf)* **211**, 240–248.
- Bassi M, Giusti H, Leite CM, Anselmo-Franci JA, do Carmo JM, da Silva AA, Hall JE, Colombari E & Glass ML (2012). Central leptin replacement enhances chemorespiratory responses in leptin-deficient mice independent of changes in body weight. *Pflugers Arch* **464**, 145–153.
- Calgani A, Monache SD, Cesare P, Vicenti C, Bologna M & Angelucci A (2016). Leptin contributes to long-term stabilization of HIF-1 α in cancer cells subjected to oxygen limiting conditions. *Cancer Lett* **376**, 1–9.
- Chen H, Charlat O, Tartaglia LA, Woolf EA, Weng X, Ellis SJ, Lakey ND, Culpepper J, Moore KJ, Breitbart RE, Duyk GM, Tepper RI & Morgenstern JP (1996). Evidence that the diabetes gene encodes the leptin receptor: identification of a mutation in the leptin receptor gene in *db/db* mice. *Cell* **84**, 491–495.
- Ciriello J & Caverson MM (2014). Carotid chemoreceptor afferent projections to leptin receptor containing neurons in nucleus of the solitary tract. *Peptides* **58**, 30–35.
- Considine RV, Sinha MK, Heiman ML, Kriauciunas A, Stephens TW, Nyce MR, Ohannesian JP, Marco CC, McKee LJ & Bauer TL (1996). Serum immunoreactive-leptin concentrations in normal-weight and obese humans. *N Engl J Med* **334**, 292–295.
- Drorbaugh JE & Fenn WO (1955). A barometric method for measuring ventilation in newborn infants. *Pediatrics* **16**, 81–87.
- Duffin J (2007). Measuring the ventilatory response to hypoxia. *J Physiol* **584**, 285–293.
- Fleury Curado T, Pho H, Berger S, Caballero-Eraso C, Shin M-K, Sennes LU, Pham L, Schwartz AR & Polotsky VY (2018). Sleep-disordered breathing in C57BL/6J mice with diet-induced obesity. *Sleep* **41**. <https://doi.org/1093/sleep/zsy089>.
- Gautron L & Elmquist JK (2011). Sixteen years and counting: an update on leptin in energy balance. *J Clin Invest* **121**, 2087–2093.
- Gonzalez-Martin MC, Vega-Agapito MV, Conde SV, Castaneda J, Bustamante R, Olea E, Perez-Vizcaino F, Gonzalez C & Obeso A (2011). Carotid body function and ventilatory responses in intermittent hypoxia. Evidence for anomalous brainstem integration of arterial chemoreceptor input. *J Cell Physiol* **226**, 1961–1969.
- Handa P, Maliken BD, Nelson JE, Morgan-Stevenson V, Messner DJ, Dhillon BK, Klintworth HM, Beauchamp M, Yeh MM, Elfers CT, Roth CL & Kowdley KV (2014). Reduced adiponectin signaling due to weight gain results in nonalcoholic steatohepatitis through impaired mitochondrial biogenesis. *Hepatology* **60**, 133–145.
- Hernandez AB, Kirkness JP, Smith PL, Schneider H, Polotsky M, Richardson RA, Hernandez WC & Schwartz AR (2012). Novel whole body plethysmography system for the continuous characterization of sleep and breathing in a mouse. *J Appl Physiol (1985)* **112**, 671–680.

- Inyushkina EM, Merkulova NA & Inyushkin AN (2010). Mechanisms of the respiratory activity of leptin at the level of the solitary tract nucleus. *Neurosci Behav Physiol* **40**, 707–713.
- Jacky JP (1978). A plethysmograph for long-term measurements of ventilation in unrestrained animals. *J Appl Physiol* **45**, 644–647.
- Jun JC, Shin MK, Yao Q, Devera R, Bevans-Fonti S & Polotsky VY (2013). Thermoneutrality modifies the impact of hypoxia on lipid metabolism. *Am J Physiol Endocrinol Metab* **304**, E424–435.
- Ling L, Olson EB, Vidruk EH & Mitchell GS (1997). Integrated phrenic responses to carotid afferent stimulation in adult rats following perinatal hyperoxia. *J Physiol* **500**, 787–796.
- Lopez-Barneo J, Ortega-Saenz P, Pardo R, Pascual A, Piruat JJ, Duran R & Gomez-Diaz R (2009). Oxygen sensing in the carotid body. *Ann N Y Acad Sci* **1177**, 119–131.
- Maffei M, Halaas J, Ravussin E, Pratley RE, Lee GH, Zhang Y, Fei H, Kim S, Lallone R & Ranganathan S (1995). Leptin levels in human and rodent: measurement of plasma leptin and ob RNA in obese and weight-reduced subjects. *Nat Med* **1**, 1155–1161.
- Mateika JH (2015). The role of high loop gain induced by intermittent hypoxia in the pathophysiology of obstructive sleep apnea. *Sleep Med Rev* **22**, 1–2.
- Messenger SA & Ciriello J (2013). Effects of intermittent hypoxia on leptin signalling in the carotid body. *Neuroscience* **232**, 216–225.
- Messenger SA, Moreau JM & Ciriello J (2013). Effect of chronic intermittent hypoxia on leptin and leptin receptor protein expression in the carotid body. *Brain Res* **1513**, 51–60.
- Mokhlesi B (2010). Obesity hypoventilation syndrome: a state-of-the-art review. *Respir Care* **55**, 1347–1362.
- Nurse CA & Piskuric NA (2013). Signal processing at mammalian carotid body chemoreceptors. *Semin Cell Dev Biol* **24**, 22–30.
- O'Donnell CP, Schaub CD, Haines AS, Berkowitz DE, Tankersley CG, Schwartz AR & Smith PL (1999). Leptin prevents respiratory depression in obesity. *Am J Respir Crit Care Med* **159**, 1477–1484.
- Pappenheimer JR (1977). Sleep and respiration of rats during hypoxia. *J Physiol* **266**, 191–207.
- Peppard PE, Young T, Barnett JH, Palta M, Hagen EW & Hla KM (2013). Increased prevalence of sleep-disordered breathing in adults. *Am J Epidemiol* **177**, 1006–1014.
- Peng YJ, Yuan G, Ramakrishnan D, Sharma SD, Bosc-Marce M, Kumar GK, Semenza GL & Prabhakar NR (2006). Heterozygous HIF-1 alpha deficiency impairs carotid body-mediated systemic responses and reactive oxygen species generation in mice exposed to intermittent hypoxia. *J Physiol* **577**, 707–716.
- Phipps PR, Starritt E, Caterson I & Grunstein RR (2002). Association of serum leptin with hypoventilation in human obesity. *Thorax* **57**, 75–76.
- Pho H, Hernandez AB, Arias RS, Leitner EB, Van Kooten S, Kirkness JP, Schneider H, Smith PL, Polotsky VY & Schwartz AR (2016). The effect of leptin replacement on sleep-disordered breathing in the leptin-deficient *ob/ob* mouse. *J Appl Physiol* **120**, 78–86.
- Pialoux V, Hanly PJ, Foster GE, Brugniaux JV, Beaudin AE, Hartmann SE, Pun M, Duggan CT & Poulin MJ (2009). Effects of exposure to intermittent hypoxia on oxidative stress and acute hypoxic ventilatory response in humans. *Am J Respir Crit Care Med* **180**, 1002–1009.
- Pichard LE, Crainiceanu CM, Pashai P, Kostuk EW, Fujioka A & Shirahata M (2015). Role of BK channels in murine carotid body neural responses in vivo. *Adv Exp Med Biol* **860**, 325–333.
- Polotsky M, Elsayed-Ahmed AS, Pichard L, Harris CC, Smith PL, Schneider H, Kirkness JP, Polotsky V & Schwartz AR (2012). Effects of leptin and obesity on the upper airway function. *J Appl Physiol* **112**, 1637–1643.
- Polotsky VY, Saldone MC, Scharf MT, Li J, Tankersley CG, Smith PL, Schwartz AR & O'Donnell CP (2004). Impact of interrupted leptin pathways on ventilatory control. *J Appl Physiol* **96**, 991–998.
- Polotsky VY, Wilson JA, Saldone MC, Haines AS, Hurn PD, Tankersley CG, Smith PL, Schwartz AR & O'Donnell CP (2001). Female gender exacerbates respiratory depression in leptin-deficient obesity. *Am J Respir Crit Care Med* **164**, 1470–1475.
- Porzionato A, Rucinski M, Macchi V, Stecco C, Castagliuolo I, Malendowicz LK & De CR (2011). Expression of leptin and leptin receptor isoforms in the rat and human carotid body. *Brain Res* **1385**, 56–67.
- Powell FL, Milsom WK & Mitchell GS (1998). Time domains of the hypoxic ventilatory response. *Respir Physiol* **112**, 123–134.
- Prabhakar NR (2013). Sensing hypoxia: physiology, genetics and epigenetics. *J Physiol* **591**, 2245–2257.
- Prabhakar NR, Kumar GK & Peng YJ (2012). Sympatho-adrenal activation by chronic intermittent hypoxia. *J Appl Physiol* **113**, 1304–1310.
- Prabhakar NR & Semenza GL (2012). Adaptive and maladaptive cardiorespiratory responses to continuous and intermittent hypoxia mediated by hypoxia-inducible factors 1 and 2. *Physiol Rev* **92**, 967–1003.
- Ribeiro MJ, Sacramento JF, Gallego-Martin T, Olea E, Melo BF, Guarino MP, Yubero S, Obeso A & Conde SV (2018). High fat diet blunts the effects of leptin on ventilation and on carotid body activity. *J Physiol* **96**, 3187–3199.
- Scott MM, Lachey JL, Sternson SM, Lee CE, Elias CF, Friedman JM & Elmquist JK (2009). Leptin targets in the mouse brain. *J Comp Neurol* **514**, 518–532.
- Shapiro SD, Chin CH, Kirkness JP, McGinley BM, Patil SP, Polotsky VY, Biselli PJ, Smith PL, Schneider H & Schwartz AR (2014). Leptin and the control of pharyngeal patency during sleep in severe obesity. *J Appl Physiol* **116**, 1334–1341.
- Shin M-K, Yao Q, Jun JC, Bevans-Fonti S, Yoo D-Y, Han W, Mesarwi O, Richardson R, Fu Y-Y, Pasricha PJ, Schwartz AR, Shirahata M & Polotsky VY (2014). Carotid body denervation prevents fasting hyperglycemia during chronic intermittent hypoxia. *J Appl Physiol* **117**, 765–776.
- Shirahata M & Fitzgerald RS (1991). Dependency of hypoxic chemotransduction in cat carotid body on voltage-gated calcium channels. *J Appl Physiol* (1985) **71**, 1062–1069.

- Shirahata M, Tang WY, Shin MK & Polotsky VY (2015). Is the carotid body a metabolic monitor? *Adv Exp Med Biol* **860**, 153–159.
- Silva AQ & Schreihof AM (2011). Altered sympathetic reflexes and vascular reactivity in rats after exposure to chronic intermittent hypoxia. *J Physiol* **589**, 1463–1476.
- Tankersley C, Kleeberger S, Russ B, Schwartz A & Smith P (1996). Modified control of breathing in genetically obese (*ob/ob*) mice. *J Appl Physiol* **81**, 716–723.
- Tankersley CG, Fitzgerald RS & Kleeberger SR (1994). Differential control of ventilation among inbred strains of mice. *Am J Physiol Regul Integr Comp Physiol* **36**, R1371–R1377.
- Teppema LJ & Dahan A (2010). The ventilatory response to hypoxia in mammals: mechanisms, measurement, and analysis. *Physiol Rev* **90**, 675–754.
- Trombetta IC, Maki-Nunes C, Toschi-Dias E, Alves MJ, Rondon MU, Cepeda FX, Drager LF, Braga AM, Lorenzi-Filho G & Negrao CE (2013). Obstructive sleep apnea is associated with increased chemoreflex sensitivity in patients with metabolic syndrome. *Sleep* **36**, 41–49.
- Tufik S, Santos-Silva R, Taddei JA & Bittencourt LR (2010). Obstructive sleep apnea syndrome in the Sao Paulo Epidemiologic Sleep Study. *Sleep Med* **11**, 441–446.
- Van Vliet BN, Chafe LL & Montani JP (1999). Contribution of baroreceptors and chemoreceptors to ventricular hypertrophy produced by sino-aortic denervation in rats. *J Physiol* **516**, 885–895.
- Villanueva EC & Myers MG Jr (2008). Leptin receptor signaling and the regulation of mammalian physiology. *Int J Obes (Lond)* **32**(Suppl 7): S8–S12.
- Yamauchi M, Hasan O, Dostal J, Jacono FJ, Loparo KA & Strohl KP (2008). Post-sigh breathing behavior and spontaneous pauses in the C57BL/6J (B6) mouse. *Respir Physiol Neurobiol* **162**, 117–125.
- Yao Q, Pho H, Kirkness J, Ladenheim EE, Bi S, Moran TH, Fuller DD, Schwartz AR & Polotsky VY (2016). Localizing effects of leptin on upper airway and respiratory control during sleep. *Sleep* **39**, 1097–1106.
- Younes M (2014). CrossTalk proposal: elevated loop gain is a consequence of obstructive sleep apnoea. *J Physiol* **592**, 2899–2901.
- Younes M, Ostrowski M, Atkar R, Laprairie J, Siemens A & Hanly P (2007). Mechanisms of breathing instability in patients with obstructive sleep apnea. *J Appl Physiol* **103**, 1929–1941.
- Yuan F, Wang H, Feng J, Wei Z, Yu H, Zhang X, Zhang Y & Wang S (2018). Leptin signaling in the carotid body regulates a hypoxic ventilatory response through altering TASK channel expression. *Front Physiol* **9**, 249.
- Zwillich CW, Sutton FD, Pierson DJ, Greagh EM & Weil JV (1975). Decreased hypoxic ventilatory drive in the obesity-hypoventilation syndrome. *Am J Med* **59**, 343–348.

Additional information

Competing interests

The authors have no competing financial and non-financial interests or other interests that might be perceived to influence the results and/or discussion reported in this paper.

Author contributions

M.S*, J.S.K.S., A.R.S. and V.Y.P. conceived and designed research; C.C.E., M.-K. S., H.P., L.J.K., S.B., L.E.P., Z.J.W. and H.-Y. Y. performed experiments; C.C.E., M.-K. S., H.P., L.J.K., L.E.P., L.P., C.G., H.-Y. Y., W.-Y. T., and V.Y.P. analysed data; C.C.E., M.-K. S., H.P., L.E.P., H.-Y. Y., W.-Y. T., J.S.K.S. and V.Y.P. interpreted results of experiments; C.C.E., H.P., L.J.K., L.E.P., H.-Y. Y., W.-Y. T. and V.Y.P. prepared figures; C.C.E. and V.Y.P. drafted the manuscript, J.S.K.S., A.R.S. and V.Y.P. edited and revised manuscript; C.C.E., M.-K. S., H.P., L.J.K., L.E.P., Z.J.W., L.P., C.G., S.B., H.-Y. Y., W.-Y. T., J.S.K.S. and V.Y.P. approved the final version of the manuscript. *M.S. is deceased.

Funding

This work was funded by the NIH R01s HL133100 to V.Y.P. and J.S.K.S., R01 HL128970 to V.Y.P. and A.R.S., R01 HL138932 to V.Y.P. V.Y.P. is also supported by NIEHS grant P50 ES018176 and EPA Agreements 83615201 & 83451001. C.C.E. was supported in part by 'Beca de estancias formativas de la Consejería de Salud de Andalucía 2017. C. Caballero Erasó. Número de expediente: EF-0128-2016'. This publication has not been formally reviewed by EPA. The views expressed in this document are solely those of the authors and do not necessarily reflect those of the Agency. EPA does not endorse any products or commercial services mentioned in this publication.